Failure Analysis of Homogeneous Material under Mechanical Loading using Extended Isogeometric Analysis

A Thesis Submitted in Fulfillment of the Requirement for the Award of the Degree of

MASTER OF ENGINEERING

in CAD/Cam Engineering

Submitted By

Vansh Bedi

801684014

Under Supervision of

Dr. Gagandeep Bhardwaj

(Assistant Professor, Mechanical Engineering Department)

Dr. Jaswinder Singh Saini

(Associate Professor, Mechanical Engineering Department)

MECHANICAL ENGINEERING DEPARTMENT

THAPAR INSTITUTE OF ENGINEERING & TECHNOLOGY

(A DEEMED TO BE UNIVERSITY), PATIALA, PUNJAB

JULY, 2018

CERTIFICATE

I, Vansh Bedi hereby declare that the work presented in this thesis entitled 'Failture analysis of homogenous material under mechanical loading using extended isogeometric analysis' in fulfillment of the requirement for the award of degree of Master of Engineering (CAD/CAM) submitted at Mechanical Engineering Departement, Thapar Institute of Engineering & Technology (Deemed to be University), Patiala is an authentic record of work carried out under the supervision of Dr. Gagandeep Bhardwaj (Assistant professor, Mechanical Engineering Department , TIET, Patiala) and Dr. Jaswinder Singh Saini (Associate professor, Mechanical Engineering Department, TIET, Patiala from August, 2017 to July 2018. The matter presented in this has not been submitted either in part or full to any other university or institute for the award of any other degree.

Vansh Bedi

801684014

Date : 05-08-2018

Dr. Gagandeep Bhardwaj

Assistant Professor

Mechanical Engineering Department

Thapar Institute of Engineering and Technology Patiala, Punjab

Dr. Jaswinder Singh Saini

Associate Professor

Mechanical Engineering Department

Thapar Institute of Engineering and Technology Patiala, Punjab

Acknowledgement

It would like to specially acknowledge and extent my heartfelt gratitude to all those who have helped me in completion of this thesis report. With the biggest contribution, I would like to thankAssistant Professor **Dr. Gagandeep bhardwaj** and Associate Professor **Dr. Jaswinder SinghSaini** for their full support and guidance.
Lastly, I would also like to thank my parents for their years of love and encouragement. They have always wanted the best for me and I admire their determination and sacrifice.

Vansh Bedi

Abstract

The fracture in any component is the main reason behind failure. Now days industry is so obsessed with the quality of product which make analysis of fracture is main concern. Many methods are introduced for fracture analysis. Finite element method is the basic for every modified approach. FEM doesn't give the exact results due to singularity at crack tip and also it's difficult to implement FEM due to need of re-meshing. Extended finite element is introduced to tackle these problems. In XFEM the enrichment function are used for crack face and tip. These functions are same as interpolation function in FEM and level set method is used to identify the enriched elements. The introduction of Isogeometric analysis revolutionize the design and FEA research. IGA bridge the gap between design and analysis by using same shape function. The NURBS basis function is mostly used in IGA because of its higher order and continuity. XFEM gives exact result but it's tedious to implement and takes more time because the number of iterations.

In this thesis, Extended Isogeometric Analysis (XIGA) is implemented to homogenous material having crack under mechanical loading, which is developed by integration of IGA and XFEM. In this also level set method is used to identify the enriched element in XIGA Here NURBS basis function is used as interpolation function within the framework of XFEM and gives same results in less time and less iteration.

Keywords: XIGA, IGA, PU, FEM, XFEM

Table of Contents

Table of Figure.....i
Nomenclature.....ii

CHAPTER 1.....1

INTRODUCTION.....1

1.1 FRACTURE MECHAICS.....2
1.2 BULK FRACTURE MECHANICS.....3
1.3 ENERGY RELEASE RATE.....4
1.4 CRACK TIP OPENING DISPLACEMENT (CTOD).....5
1.4.1 First-order CTOD.....5
1.4.2 Second-order CTOD.....6
1.5 J-INTEGRAL.....6
1.6 ISOGEOEMERIC ANALYSIS (IGA).....7
1.7 B-SPLINE.....8
1.7.1 Knot Vector.....8
1.7.2 Basis functions.....8
1.7.3 B-spline curve.....9
1.8 REFINEMENTS IN BASIS FUNCTION.....10
1.8.1 h-refinement: knot insertion.....10
1.8.2 Order Elevation.....10
1.8.3 k-refinement.....11
1.8.4 B-spline surface.....11
1.9 NON-UNIFORM RATIONAL B-SPLINE.....11
1.10 ISOGEOMETRIC ANALYSIS VS FINITE ELEMENT METHOD.....12
LITERATUR REVIEW.....14
2.1 INTRODUCTION.....14
2.2 FRACTURE MECHANICS.....14
2.3 MESHING METHODS.....15
2.4 MESH-LESS METHODS.....15
2.5 XIGA.....17

CHAPTER 3.....19

FORMULATION AND METHODOLOGY.....19

3.1 GENERALISATION OF J.....19
3.2 FIELD EQAUTION FOR SIFs.....19

3.3 FINITE ELEMENT METHOD (FEM) 20
3.4 PUFEM 21
3.4.1 Methodology of partition of unity with in FEM 22
3.5 XFEM 22
3.6 NURBS USED FOR ANALYSIS 24
3.7 SPACE AND MAPPINGS 24
3.7.1 Physical space 25
3.7.2 Control mesh 25
3.7.3 Parameter space 25
3.7.4 Index space 25
3.7.5 Parent element 26
3.8 ISOGEOMETRIC FORMULATION FOR LINEAR PROBLEMS 26
3.8.1 Finite element discretization 26
3.9 SOLVING THE DISCRETE PROBLEM 28
3.10 ESSENTIAL BOUNDARY CONDITIONS 29
3.11 SELECTION OF ENRICHED NODES 30
3.12 INTEGRATION 31
3.13 Difficulties in the XFEM 32
3.15 MODELING OF CRACKS IN XIGA 35
3.16 INTERACTION INTEGRAL FOR MECHANICAL LOADING 36
3.17 Crack propagation rate 37
CHAPTER 4 38
NUMERICAL RESULTS AND DISCUSSION 38
4.1 CRACK GROWTH IN HOMOGENEOUS MATERIAL 38
4.1.1 Edge crack growth 38
4.1.2 Center crack growth 41
CHAPTER 5 45
5.1 CONCLUSION 45
5.2FUTURE SCOPE 45
REFERENCES 48

Table of Figure

Figure 1.1 Modes of fracture 2

Figure 1.2 CTOD estimation in material having crack 5

Figure 1.3 Definition of J integral around a crack and equivalent to domain A^*. 6

Figure 1.4 Basis function of order 0,1,2 for uniform knot vector [25] 9

Figure 1.5 Quadratic basis functions for open, non-uniform knot vector $\Xi = \{0,0,0,1,2,3,4,4,5,5,5\}$. 9

Figure 1.6 (a) Projective transformation of control points (b) Projective transformation of B-spline curve $C^w(\xi)$ with NURBS curve $C(\xi)$ 12

Figure 3.1 Finite Element method of analysis 23

Figure 3.2 Partition of unity method 25

Figure 3.3 Standard interpolation functions on domain 26

Figure 3.4 Mapping between spaces 27

Figure 4.1 Edge cracked homogenous body with loading and boundary conditions 41

Figure 4.2 Convergence of (a) XIGA and (b) XFEM for an edge crack in homogenous material 42

Figure 4.3 K_I variation with crack extension for an edge crack in homogenous material 42

Figure 4.4 Crack growth path for an edge crack in homogenous material 43

Figure 4.5 (a) Contour plot of σ_{yy} (MPa) for an edge crack in homogenous material, (b) Contour plot of ε_{yy} for an edge crack in homogeneous material 44

Figure 4.6 Center cracked homogenous body with loading and boundary conditions 44

Figure 4.7 K_I variation with crack extension for a center crack in homogenous material 45

Figure 4. 8 Convergence of (a) XIGA and (b) XFEM for a center crack in homogenous material 45

Figure 4.9 Crack growth path for a center crack in homogenous material 46

Figure 4.10 (a) Contour plot of σ_{yy} (MPa) for a center crack in homogenous material, (b) Contour plot of ε_{yy} for a center crack in homogenous material 46

Nomenclature

G	Energy release rate
G_c	Fracture toughness of material
K	Stress intensity factor
J	J-integral
E	Young's modulus
W	External work on plate
U	Elastic energy
A	Crack length
W_s	Strain energy density function
P	Polynomial order
N	Number of basis functions
N	B-spline basis function
C	B-spline curve
S	B-spline surface
R	NURBS basis function
M	Multiplicity of knot
u(x,y)	Displacement trial solution
b(x,y)	Body force
D	Displacement at control point
B	B matrix
R^e	Element shape function matrix
u^e	Element displacement trail solution
d^e	Displacement matrix for parent element
n_{el}	Number of elements
J	Jacobian matrix
D	Compliance matrix
K	Global stiffness matrix

Greek Symbols

σ	Stress
ε	Strain
κ	Kolosov constant
μ	Shear modulus
ν	Poisson's ratio
Γ	Energy required to grow crack
Ω	Domain around crack
θ	Angle between crack tip and node
Ξ	Set of knot vector
ξ	Knot vector in x-direction
η	Knot vector in y-direction
γ	Shear strain
λ	Lagrange multiplier

ϕ	Interpolation function

Acronyms

SIF	Stress intensity factor
CTOD	Crack tip opening displaement
NURBS	Non-uniform rational B-spline
PU	Partition of unity
EFGM	Element free Glakerin method
IGA	Isogeometric analysis
FEM	Finite element method
XFEM	Extended finite element method
PUFEM	Partition of unity finite element method
LEFM	Linear elastic fracture mechanics
XIGA	Extended isogeomtric analysis
LSM	Level set method

CHAPTER 1

INTRODUCTION

It is important to assure the safety of every component. As the world grows, every consumer is concerned about quality of product and its top most priority of manufacture to design better quality product. To insure the quality of the product every industry analyzes it before manufacturing. In the today world due to advancement in the computational system now it's easy and convenient to analyze. The fracture failure is most prioritized because mostly components are failed due to propagation of crack in it. It is hard to analyze failure in any material or component. The failure due to fracture is the main concern. To solve the problems of fracture mechanics several researchers developing different approaches through decades. Because of complexity of problem and singularity at crack tip the FEM can't give the accurate results and also these methods are time consuming. So then the new approach is introduced XFEM which is very popular in the modeling of crack.

It is based on PU method that helps to model the crack without the help of FEM but it used the FEM framework with enrichment functions tip length by solving the singularity of crack tip. This is capable to solve higher order discontinuity problems. Unlike in FEM there is no need to re-meshing in XFEM also the enrichment is easy and less time consuming way to solve problems. The XFEM is also used to solve the problems of defects like holes and inclusion etc. For tracking of discontinuity level set method is used. But still the formulation of XFEM use to approximate for getting results and no exact geometry is defined which is then solved by the discovery of IGA approach by Hughes *et al.*[36] in 2005.Which uses same basis function both for geometry modeling and analysis. From then implementation of IGA is done into every field due to its easy approach and less convergence potential. To implement IGA to fracture analysis a new approach is proposed which is combination of IGA and XFEM called extended Isogeometric analysis (XIGA). In this the framework of XFEM is used with same basis function of IGA. Mainly in IGA the basis function of NURBS curve are used because of its ability to model exact geometry and it's easy to use in analysis part.

1.1 FRACTURE MECHAICS

The failure in any material is because of many factors like yielding, buckling, fatigue, fracture, creep, vibration modes and impact. Fracture is our main concern. Fracture is the cracking or breaking of a hard object or material which cause failure. The material is mainly divided into two types brittle and ductile. Both have different due to fracture. In brittle material crack moves easily. Ductile fracture causes plastic deformation at large amount to a significant depth. Brittle fracture classified into two groups: Inter-granular and trans-granular. Inter granular crack moves along grain boundaries and in trans-type crack moves within grains. Ductile fracture growth takes place because of plastic deformation and due to micro-voids.

There are three modes of fracture failure as shown in Figure 1.1. Mode I is opening mode in which crack surface have displacement which is normal to it. Mode II is sliding mode because of displacement occur in the plane of plate just opposite in mode III the displacement is parallel to crack front, having tearing in it. Mode-I is mostly dominant in engineering application of failure and appeared most dangerous. In certain cases mode-II and mode-III are also cause failure in material.

There are parameters to define the intensity of crack. The mostly four parameters are used to calculate the potency of crack. Energy release rate (G), CTOD, J-integral and SIF.

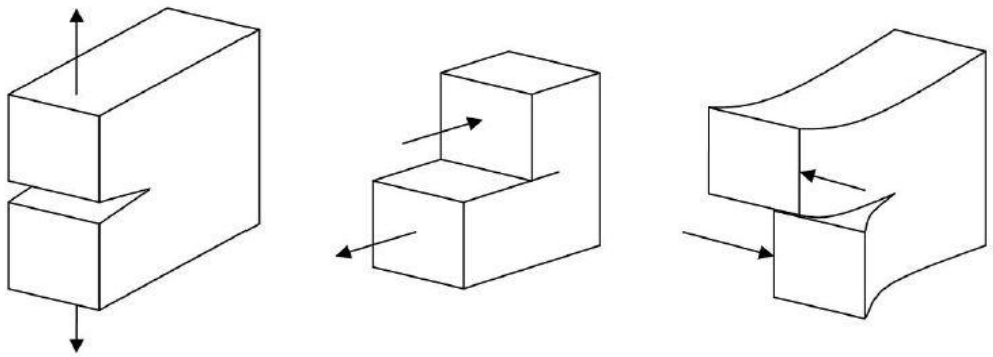

Mode I Mode II Mode III

Figure 1.1 Modes of fracture [55]

1.2 BULK FRACTURE MECHANICS

Displacement, strain and stress field becomes independent to the geometry of specimen as it gets closer to the crack tip. For fields near the crack tip characterised by the three SIF values - K_I, K_{II} and K_{III} to the mode as explained. The SIFs are related to traction force and distance *r* from crack tip by [55]

$$\left(\sigma_{22} + i\tau_{12}\right)_{\theta=0} = \frac{K_I + iK_{II}}{\sqrt{2\pi r}} \tag{1.1}$$

The *r* and θ are shown in Figure 1.2. The amount relative from mode II to mode I loading on specimen is calculated by mode angle [55]

$$\psi = \tan^{-1}\left(\frac{K_{II}}{K_I}\right)$$

For mode angle zero the loading be pure mode I and at angle 90^o become pure mode II. The displacement near crack tip expressed as follows [55]

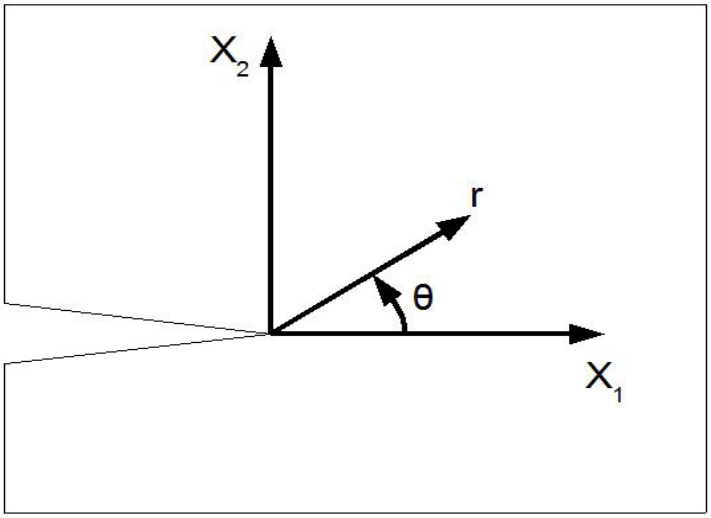

Figure 1.2 Crack tip based coordinates system. [55]

$$u = (u_x^I) + (u_x^{II}) + (u_y^{II}) - (u_y^{II}) \tag{1.2}$$

$$
\begin{aligned}
u_x^I &= \frac{K_I}{2\mu}\sqrt{\frac{r}{2\pi}}\cos\left(\frac{\theta}{2}\right)\left[k-1+2\sin^2\left(\frac{\theta}{2}\right)\right] \\
u_x^{II} &= \frac{K_{II}}{2\mu}\sqrt{\frac{r}{2\pi}}\cos\left(\frac{\theta}{2}\right)\left[k+1+2\sin^2\left(\frac{\theta}{2}\right)\right] \\
u_y^I &= \frac{K_I}{2\mu}\sqrt{\frac{r}{2\pi}}\cos\left(\frac{\theta}{2}\right)\left[k+1-2\sin^2\left(\frac{\theta}{2}\right)\right] \\
u_y^{II} &= \frac{K_{II}}{2\mu}\sqrt{\frac{r}{2\pi}}\cos\left(\frac{\theta}{2}\right)\left[k-1-2\sin^2\left(\frac{\theta}{2}\right)\right]
\end{aligned}
\qquad (1.3)
$$

$$\kappa = 3-4\mu$$

$$\mu = \frac{E}{2(1+\nu)}$$

Where κ and μ are Kolosov constant and shear modulus, respectively. The displacement and stress fields are asymptotic in nature. So it clears that stresses go to the value infinity as comes to crack tip. For crack in perfectly elastic material the equations below give asymptotic solution. The region is affected by boundary condition has been far from the crack tip. At close to the crack tip there is region of infinite stresses and in between these two there is a region where k dominant. The linearity and elasticity still hold as property. In this area the fields governed by stress intensity factor. There are also other methods to characterize the crack one of important method is energy method or energy release rate.

1.3 ENERGY RELEASE RATE

The energy release per unit area during crack propagation is called energy release rate. It's denoted by symbol G. the value of G is shown by Griffith energy balance [55].

$$\frac{dW}{da} - \frac{dU}{da} = \frac{d\Gamma}{da} \qquad (1.4)$$

where *W* is external work, *U* is elastic energy, Γ is energy to grow the crack and 'a' is crack length. Value of G is obtained by equation and crack grows when the value of G become greater than G_c (fracture toughness of material). The stress SIF and energy release rate related to each other as [55]

$$G = \frac{\left(K_I^2 + K_{II}^2\right)}{\overline{E}} \qquad (1.5)$$

Where $\bar{E} = \frac{E}{(1-\nu^2)}$ (for plane strain)

The failure analysis of structure having crack under different loads is the Study of fracture mechanics. For analysis of crack we have to calculate SIF value which is the substantial parameter in fracture mechanics. Therefore different methods are developed for the calculation of SIF. The accurate value of is must for further prediction of life of component having crack. There are methods to develops formulation is categorized under two types. The energy based and displacement based. In displacement based methods the displacement near the crack tip is used under asymptotic expansion.

It relates the stress filed value with energy release rate. By using the definition of J-integral is used to calculate the value of energy release rate. The calculation of G in the two dimensional crack is basically J-integral method. J-integral is path independent integral equals to rate of change of potential for unit extension of crack

1.4 CRACK TIP OPENING DISPLACEMENT (CTOD)

This is different approach from the others, this is used for elasto plastic behaviour and for ductile fracture around the crack tip been proposed by Cotrell *et al.* [46] in 2006. As in LEFM are taken in the case of brittle fracture and CTOD is always zero for brittle fracture. The use of CTOD in ductile fracture is because of large deformation crack as shown in Figure 1.3. For determining the value of CTOD there are two approaches first and second order explained below

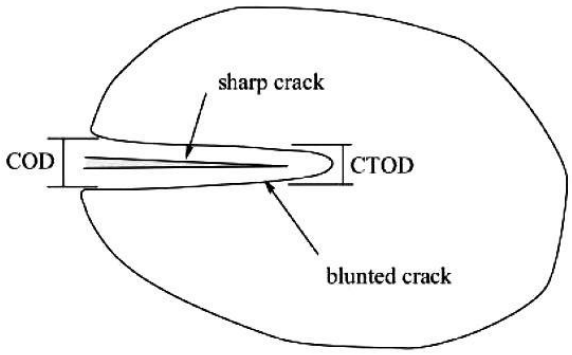

Figure 1.2 CTOD estimation in material having crack. [55]

1.4.1 First-order CTOD

The Irwin's solution is used to define the CTOD solution. The COD (crack tip opening) evaluated as follow at a distance *r* [55]

$$COD = 2\mu_y = \frac{\kappa+1}{\mu} K_I \sqrt{\frac{r}{2\pi}} \tag{1.6}$$

Taking, $r = r_p$ where r_p is in plastic zone, then crack tip opening is

$$CTOD = \frac{4}{\pi} \frac{K_I^2}{E\sigma_{yld}} \tag{1.7}$$

1.4.2 Second-order CTOD

CTOD formulation for second-order has been proposed by Kanninen [55]

$$CTOD = \frac{K^2}{E\sigma_{yld}} \tag{1.8}$$

Taking $G = K^2 / E$ by the definition of energy release rate.

$$CTOD = \frac{G}{\sigma_{yld}} \tag{1.9}$$

1.5 J-INTEGRAL

Consider a circle around crack tip. By this approach of domain integral the j-integral converting from line integral to area integral under the area of circle. By this method, domain integral is derived for homogenous material under the thermal stress.

Path independent line integral is defined as

$$J_{\underline{k}} = \lim \int (W_s n_k - \sigma_{ij} n_j u_{i,k}) d\Gamma \tag{1.10}$$

where, W_s is mechanical strain energy density function.

$$W_s = \int_0^{\varepsilon} \sigma_{ij} d\varepsilon_{ij} \tag{1.11}$$

where, n_k is outward normal to Γ_e and σ_{ij} is stress component.Γ is counter-clockwise closed contour, $d\Gamma$ is differential element along crack path $t = \sigma.n$ is traction vector on a plane where *n* is normal outward to plane and *u* is displacement vector as shown in Figure 1.4.

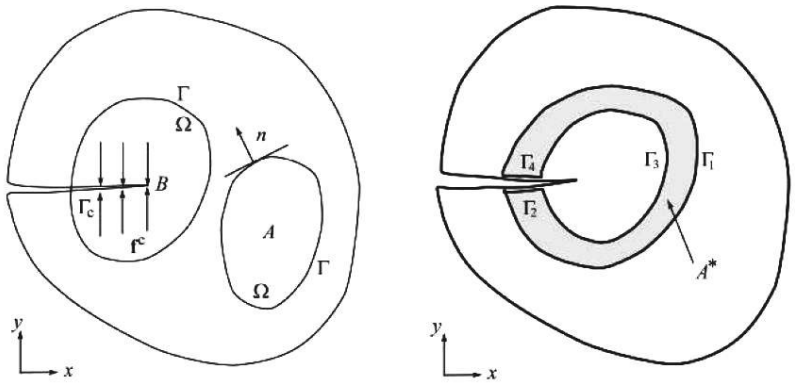

Figure 1.3 J-integral around crack within the domain [55]

For understanding of cracks consider a body under continuous stress as shown in Figure 1.4 the closed path $\Gamma = \Gamma_1 + \Gamma_2 + \Gamma_3 + \Gamma_4$ is constructed, where first two are arbitrary contour and other two are place on opposite face of traction free crack.

$$J = J_{\Gamma_1} + J_{\Gamma_2} + J_{\Gamma_3} + J_{\Gamma_4} = 0 \tag{1.12}$$

It indicated that the value of J-integral remains identical over arbitrary paths. The contour begins from one crack surface to other face used to calculate the J-integral. The shape and size selection of curve is depends to the geometry of crack.

J-integral is equals to potential energy change as per unit crack extension da. This is defined as

$$\prod = \int_{\Omega} W_s d\Omega - \int_L t_i u_i d\Gamma \tag{1.13}$$

Hence J-integral related to potential energy as

$$J = -\frac{d\prod}{da} \tag{1.14}$$

This approach is not suitable for calculation of stress and strain. So it is important to convert line integral to domain integral around crack tip. To define domain integral first have to define area around crack tip which should be a circle.

1.6 ISOGEOEMERIC ANALYSIS (IGA)

IGA used same function for both design and analysis part, and basis function are totally dependent on geometry of structure. The NURBS basis functions are basically used in it and

classical FEM is used as analysis tool. This method narrows the gap between design and analysis. Make the things easier. The NURBS are built from B-spline. To understand NURBS first take a look at B-spline.

1.7 B-SPLINE

B-spline having piecewise polynomial functions. At the interval boundaries we require function to be continuous. The B-splines curves are continuous, differentiable and smooth. These curves are most suitable for the geometry.

1.7.1 Knot Vector

NURBS curve is derived from B-splines which is local to sub domains having models which are uniform. A knot vector in parametric space is one dimensional set of coordinates.

$\Xi = [\xi_1, \xi_2, \ldots\ldots \xi_{n+p+1}]$ where n is number of basis function and p is polynomial order which comprise the B-spline.

The order p=0, 1, 2 and 3 so on refers to constant, quadratic, cubic etc. The order is computational geometry degree. Uniform knots vectors are equally spaced just opposite unequally spaced are called non-uniform knot vectors. Repeated knot vector are those which can located at same coordinates.

1.7.2 Basis functions

B-spline basis functions are defined repetitively starting with piecewise constants taking p=0. [56]

$$N_{i,p}(\xi) = \begin{cases} 1 & if \quad \xi_i \leq \xi \leq \xi_{i+1} \\ 0 & otherwise \end{cases} \tag{1.15}$$

For p= 0, 1, 2…

$$N_{i,p}(\xi) = \frac{\xi - \xi_i}{\xi_{i+p} - \xi_i} N_{i,p-1}(\xi) + \frac{\xi_{i+p+1} - \xi}{\xi_{i+p+1} - \xi_{i+1}} N_{i+1,p-1}(\xi) \tag{1.16}$$

The Figure 1.4 shows the results of equations (1.15) and (1.16) for a uniform knot vector. The basis functions having same value as standard piecewise constant and linear element function for p=0 and 1. But basis functions for p>1 are different than quadratic finite element functions these basis function. This thing will be same as move to higher order functions and easy to solving equations over finite element functions.

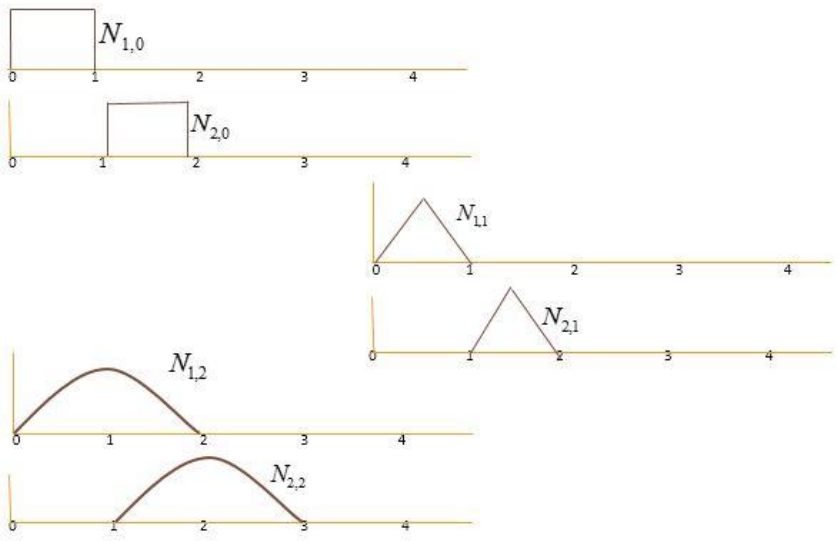

Figure 1.4 Basis function of order 0, 1, 2 and 3 for uniform knot vector [56]

An example for quadratic basis functions having open, non-uniform knot vector is shown in Figure 1.5. Basis functions are continuous derivatives of order *p* and *p*-1. The number of continuous derivatives can be decreased by *j* when knot is repeated by same value.

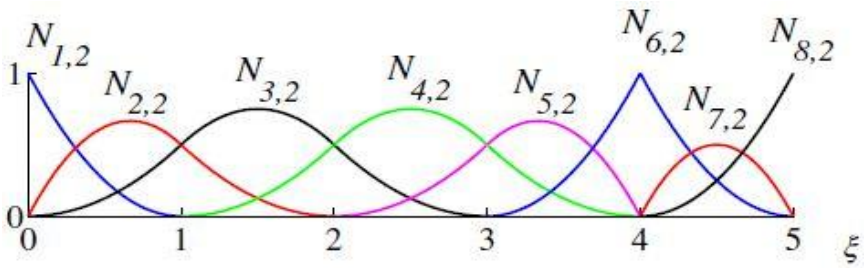

Figure 1.5 Quadratic basis functions for non-uniform open knot vector [56] $\Xi = \{0,0,0,1,2,3,4,4,5,5,5\}$.

The properties of B-spline basis functions are:

1. They based on PU
2. The support of each basis function is contained is compact and in interval.
3. Coefficient of mass matrix computed from B-spline basis function is greater than, or equal to zero.

1.7.3 B-spline curve

Linear combination of B-spline basis functions are used to construct B-spline curve R^d. The coefficient of functions is referred as control points. Given *n* as basis functions from 0 to *n*, and corresponding control point $B_i \in R^d$ a piecewise-polynomial B-spline curve is given by [56]

$$C(\xi) = \sum_{i=1}^{n} N_{i,p}(\xi) B_i \tag{1.17}$$

The properties of B-spline curves are:

1. They have continuity of order $p - 1$ in the absence of repeated knots.
2. The continuous derivative decrease by the same times as a knot repeats.
3. Have the property of affine covariance.

1.8 REFINEMENTS IN BASIS FUNCTION

1.8.1 h-refinement: knot insertion

In knot insertion, without changing curve geometrically knots are inserted. Given a knot vector $\Xi = \{\xi_1, \xi_2, \xi_3 ..... \xi_{n+p+1}\}$. For n+1 order basis functions are formed let $\bar{\xi}$ is the new knot. The new basis function are formed by [56]

$$\bar{B}_i = \alpha_i B_i + (1 - \alpha_1) B_{i-1} \tag{1.18}$$

where

$$\alpha_i = \begin{cases} 1 & 1 \le i \le k - p \\ \dfrac{\bar{\xi} - \xi_i}{\xi_{i+p} - \xi_i} & k - p + 1 \le i \le k \\ 0 & k + 1 \le i \le n + p + 2 \end{cases} \tag{1.19}$$

In this knot vectors repeated and continuity of curve reduced. But knot vector may not repeated p times because then curve becomes discontinues. Where a new knot $\bar{\xi}$ =0.5 is inserted. The new curve is geometrically same after insertion but the basis function and control points are changed. So basically this is used to add more basis functions of same order without changing curve.

1.8.2 Order Elevation

The order elevation is same as p-refinement in FEM approach. The polynomial order of curve is increasing without changing the geometry. The number of new control points is depends upon the multiplicities of existing knots. For doing this divide the curve into many curves. Then remove the knot to combine those segment curves into one. In this multiplicity is increased by

one. Also the control points and basis function increased by one and location of control points changed without changing the geometry of curve.

1.8.3 k-refinement

When another knot vector $\bar{\xi}$ is inserted between two knot vectors of order p in curve, the number of continuous derivate is $p - 1$. To preserve the discontinuity of curve the multiplicity of curve can increase. Let the order of curve be changed to new order q.

1.8.4 B-spline surface

B-spline also use basic concept of B-spline curve. There is another knot vector to define surface. For a control net B_{ij} where i=1,2,3….n and j=1,2,3…m having knot vectors $\xi = \{\xi_1, \xi_2 ..... \xi_{n+p+1}\}$ And $\eta = \{\eta_1, \eta_2 ..... \eta_{m+q+1}\}$. Where p and q are polynomial orders. So the surface is defined as [56]

$$S(\xi,\eta) = \sum_{i=1}^{n}\sum_{j=1}^{m} N_{i,p} M_{j,q} B_{i,j} \tag{1.20}$$

1.9 NON-UNIFORM RATIONAL B-SPLINE

By projective transformations of B-spline entities desired geometric entities in R^d can be obtained in Figure 1.6. In particular, conic sections, such as circles and ellipse, by projective transformations of piecewise quadratic can be exactly constructed curves. The projective transformation of a B-spline curve yields a rational polynomial of the form $C_R(\xi) = f(\xi) / g(\xi)$.

Where f and g are piecewise polynomials. The rational B-spline curve construction is shown in Figure 1.6 proceeds as follow. Let $\{B_i^w\}$ be a set of control points. For a B-spline in R^{d+1} with knot vector Ξ these are referred to as the “projective” control points for NURBS curve in R^d. [56]

$$R_i^p(\xi) = \frac{N_{i,p}(\xi) w_i}{\sum_{i=1}^{n} N_{\hat{i},p}(\xi) w_i} \tag{1.21}$$

$$C(\xi) = \sum_{i=1}^{n} R_i^p(\xi) B_i \tag{1.22}$$

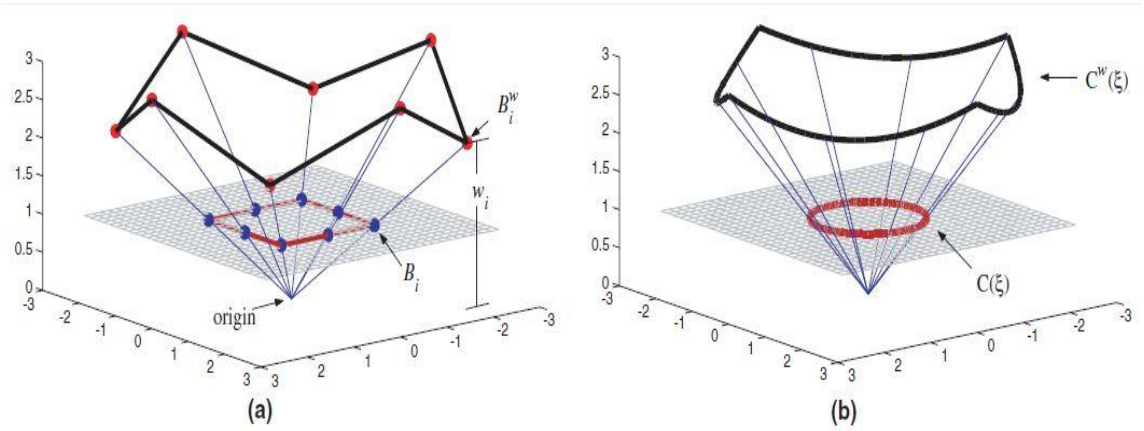

Figure 1.6 (a) Projective transformation of control points (b) Projective transformation of B-spline curve [56]

Important properties of NURBS are:

1. Basis functions of NURBS form a partition of unity.
2. The continuity and support of NURBS basis function are same as B-splines.
3. It have property of affine covariance after transformation to the control points.
4. NURBS becomes B-spline, when weights are equal

1.10 ISOGEOMETRIC ANALYSIS VS FINITE ELEMENT METHOD

Table 1.1 Differences between FEA and IG

IsogeometAric analysis	Finite element analysis
Control points	Nodal points
Control variable	Mesh
Exact geometry	Approximated geometry
Knots	Mesh
NURBS basis functions	Lagrange basis function
Patches	Sub domains
Basis not interpolating control points	Basis interpolating nodes

There are some differences and similarities between Isogeometric analysis and standard FEM is shown in Table 1.1. In IGA the same basis function is used for defining the exact

geometry and for analysis. In classical FEM the basis functions used to approximate the unknown solution field. NURBS based Galerkin FEM is somewhat similar to FEA.

For Isogeometric analysis we do not need FEM mesh and nodal points as input for geometry, we need knots vector and control points. The connectivity array is also different in IGA as it links global shape function from the local shape function. The connectivity array is found out by the knot vectors and polynomial orders same as for global stiffness matrix. That how both matrix are different as in classical FEM.

In IGA exact geometry is employed at all discretization levels. For FEM we have to apply piecewise polynomial and give description of geometry. But in IGA we do not need to explain geometry to analysis that's providing great accuracy to solution in IGA. As in FEM the solution of approximate is linear combination of basis function. In FEM the interpolation is done on control pints and control variable unlike in IGA it be on nodal points. Both methods are implementation of iso parametric approach given in Galerkin method. In IGA the NURBS functions are only positive unlike in FEM the basis functions can be negative and positive. Degree of freedom are locates at nodes in FEM while in IGA located at control points

CHAPTER 2

LITERATUR REVIEW

2.1 INTRODUCTION

The main and uncertain reason of failure of any material or component is the propagation of fracture in it. The fracture shows discontinuity during the analysis. It is always remained challenge in the computational mechanics. In the starting of analysis the discontinuity like crack is modeled by the FEM in which mesh refinement is mandatory to find out the true stress field around crack. This refinement approach is first used by Swenson and Ingraffea in 1988 [1]. In this re-meshing is done near crack. This approach is difficult to solve in case of dynamic crack propagation because of generation of new mesh every time and also need to calculate the shape functions every time. This process also results in loss of accuracy. Due to complexity of problem and less convergence rate around crack tip Belytschko *et al.* [2] introduced XFEM which have special enrichment function for crack length and crack tip. After the introduction of Isogeometric analysis by Hughes *et al.* in 2005 [3] which uses same shape function for design and analysis and by the integration of XFEM and IGA the new approach is made called extended Isogeometric analysis (XIGA).

2.2 FRACTURE MECHANICS

The material strength to resist fracture is inherent property. So it's important to design a component, which ensure stresses produce in it should not be more than fracture stress by Bazant and Planas 1997 [4]. The Griffith in 1924 [5] was the first who introduced the effect of crack in material. His theory shows how propagation of fracture is the reason of lower tensile strength also derived the relationship between crack size and fracture strength.

The Griffith's [6] theory is used to solve the problem of plate having infinite length for elliptical and circular holes. Westergaard [7] introduced a solution for cracks by degeneration into straight crack of elliptical hole and also derived solutions for stress field near crack tip. Irwin *et al.* [8] introduced the concept of SIF and energy release rate G. Wells *et al.* [9] introduced concept of crack opening displacement as strength parameter of crack.

The concept of J-integral was introduced by Rice [10] which opened to use finite element solution for fracture problems. From then FEM has been used for many fracture problems which originally used as analytical tool for obtaining stress and displacement fields. The singularity at

crack was introduced by Barsoum [11]. Fawkes *et al.* [12] gave the simulation numerical technique of singularity at crack tip.

2.3 MESHING METHODS

The element deletion method is another method for simulation of crack introduced by Beiseel S and Belytschko [13] in 1998. In this method discontinuities modeled by constitutive relationship which is modified in element of crack.

Earlier Koh *et al*. [14] introduced Euler Lagrangian kinematic equation for dynamic crack propagation analysis in 1986 to improve the results and accuracy from previous methods like by Kanninen *et al*. [15] in which analysis at crack tip is complicate and shows inaccurate results. Also in Euler Lagrangian in this adjust mesh due to change in crack extension. This is also use triangular quarter point parametric approach due to singular field near crack tip introduced by Swenson D and Ingraffea [16].

2.4 MESH-LESS METHODS

Belytechko T *et al*. [17] introduced Galerkin method (GM) in 1996 which doesn't require re-meshing. Crack propagation equation in this method it's difficult to adjust the crack path direction and speed of crack growth constantly because for this limitation the value of SIF becomes equal to dynamic fracture toughness.

The global-local methodologies introduced for enriching the approximation filed. The idea behind this approach is to get result by global solution using coarse meshing and find out the result of discontinuities by localization used in 1986. The first utilizing of enrichment in crack problems is by Gifford *et al.* [18] in 1978 by the combination by FEM polynomial displacement and enriched displacement.

The pioneer in using of local enrichment of approximation field is done by Belytschko *et al.* [19] named this approach as Embedded finite element method (EFEM). The three field displacement, strain and stress are enriched within the same framework. The main feature of this method is localized element level enrichment. It uses the PU approach for enrichment of approximation field.

In 1999 the Belytschko and Black [20] developed the new approach is called extended finite method (XFEM) which is able to the enrichment of the approximation space within framework of FEM. It has capacity to get results with optimal convergence rate. Modeling of

complicated domains is very difficult with the standard FEM because the meshing is required to align with domain boundaries. So for tackle this mesh less method is needed. The Element Free Galerkin mehod (EGF) is one of independent method. The field is approximated by shape functions or moving least square functions. The detailed theory and application is defined in Liu *et al.* [21].

The PU was first explained by Duarte and Oden [22] in 1996. The approach is to define set of function over a domain such that the sum of functions is one. This property is essential for convergence. In same year of 1996 Strouboulis *et al.* [23] applied the concept of partition of unity in the framework of FEM and it's called PUFEM. This methods use Lagrangian basic function and FEM elements sharing the same nodes for nodal shape function which generate a non-smooth, non-polynomial function into approximation space. It make possible to approximate the field locally. In the series of mesh less method there is another method EEFG introduced by Flemmin *et al.* [24] in 1997. In 2000 Strouboulis *et al.* [25] used the same concept of partition of unity and introduced the new method GFEM which embedded different PoU function into finite element approximation to locally enrich the field.

Belytschko and Black [26] developed a method which laterXFEM modified as to enrich the field locally using partition of unity. They proposed this method for crack propagation method. The multiplication of enrichment function with the standard finite element basis functions. Constructed enriched basis function. The analytical solution for the displacement field and stress field near the crack tip is calculated by the theory of LEFM. So for enriching the field near the crack it use tip enrichment function through length.

Modification of this named as XFEM is proposed by Moes *et al.* [27] which removed the need for minimal mesh refinement. As the function used describes the field into approximate space and less dependence on analytical solution make it different from earlier version GFEM. It makes more flexible, two types of enrichment functions were proposed for the crack propagation problems. This help to approximate high strain/stress gradient fields near the crack tip. In this case the number of enrichment function is equal to number of degree of freedom. The main approach is to apply the enrichment locally. In XFEM the problem is subdivided into two parts A) Generating mesh without cracks. B) Enriching the FEM approximation models the discontinuities with additional functions.

Also in 2000 Sukumar *et al.* [28] applied the XFEM for modeling of 3D crack propagation. XFEM experienced another improvement when it coupled with Level set method by Stolarska *et al.* [29]. LSM is numerical technique to track the discontinuities which was introduced by Osher and fedkiw [30]. In level set the discontinuity is defined as zero and it help to defining in crack tip polar coordinate system for the position of point. It evaluates the distance function and step function for modeling for strong and weak discontinuities respectively. The Sukumar *et al.* [31] couple the FMM to three dimensional implementation of XFEM.

Due to possibility of defining the discontinuities, XFEM is also applied for modeling of holes and inclusion, which is difficult by standard FEM because of requirement to align the geometry. For cases where process zone is taken into account traction-separation law is used so Moes and Belytschko [32] provided a method using the framework of XFEM for cohesive crack growth.

In 2003 Zi and Belytschko [33] proposed a new element where entire crack is enriched by one enrichment function. In their approach they enrich the nodes using sign functions which are cut by crack. Meschke and Dumstorff [34] proposed a global energy method within frame work of XFEM for modeling of cohesive crack in brittle and quasi brittle material.

2.5 XIGA

In 1993 Sachramm and WD pilkey [35] introduced CAD in FEM. NURBS and Gordan surface directly used for mapping of the FEM approach and for the optimization of the structural shape.

Trying to narrow the gap between design and analysis; Hughes *et al.* [36] in 2005 suggested IGA as an alternative to FEM. They give way to use NURBS as basic for analysis which is used as free form modeling in computer graphics. Or say NURBS function in IGA used to define the geometry and for solving the solution. From then utilization of IGA is being successful in many engineering problems and implemented by many researcher for different problems. Wall *et al.* [37] and Manh *et al.* [38] used it in shape optimization. To solve problems like shell analysis Uhm and Youn [39] in 2009 used IGA. In recent years, IGA has been extended to solve fracture problems. In series of fracture analysis by IGA approach there are some following researcher whose implement IGA with the integration with XFEM in fatigue analysis. In 2012 Ghorashi *et al.* [40] and De Luycker *et al.* [41] introduced XIGA form which

incorporating the enrichment technique of IGA within framework of XFEM to model crack face continuity.

For analysis of thermal loading on crack face there are several researcher use numerical methods like Wilson and Yu [42] and Prasad *et al.* [43]. Then in 2013 Hosseini *et al.* [44] and Mohammadi [45] for analyze of fracture used XFEM. There are several researcher use numerical methods for thermal loading problems

J.A Cotrell *et al*. [46] used Isogeometric analysis for structural components for better and accurate results. A Wall *et al*. [47] introduced IGA in structural shape optimization for which efficient geometry control together by NURBS functions with smooth boundaries also applied for vibration analysis for higher order problems and discontinuities compare it with experimental results. Borden *et al*. [48] adaptive analysis with use of local h-refinement with T-Splines because NURBS only use rectangular grid of control points in parametric space straight forward a posterior error estimator local refinement of meshes.

S Ghorashi *et al*. [49] used XFEM for simulation of stationary and propagation cracks can reproduce discontinuity across a crack and crack tip singular fields. For improving the accuracy of integration the sub triangular technique is utilized from Gauss quadrature rule. I.V Singh *et al*. [50] introduced the fatigue crack growth numerical simulation using XFEM. Fatigue crack under cyclic growth law of loading standard Paris fatigue crack is used for the life elimination analysis on plate having multiple discontinuities. Gracie R *et al.* [51] used the XFEM for elaborate crack propagation modeling geometrically in brittle material. Other than that Michael J Borden *et al*. [52] give phase field of variation formulation for brittle material using IGA concept which prove complex crack behavior in both 2D and 3D component which is known as four phase theory. Use of IGA approach is now utilized in many mechanical and medical problems also. From 2012 there were many researchers whose implemented IGA instead of traditional methods for getting better results as such Borden developed phase field model of higher order for brittle fracture using IGA. Other than fracture the Isogeometric analysis implemented by S. Morganti *et al*. [53] in the field of medical as structural analysis of valve closure.

CHAPTER 3

FORMULATION AND METHODOLOGY

3.1 GENERALISATION OF J

To analysis the fatigue growth, the SIF is the main parameter to represent the crack growth. To obtain value of SIF, first need to calculate the j-integral. There are various methods proposed to calculate the j-integral. The incompatibility formulation is best among because less derivation is used with more level of accuracy.

The original definition of J can be defined as [45]

$$J_k = \int_\Gamma \left\{ W_s \eta_k - t \frac{\partial u}{\partial x_k} \right\} d\Gamma \tag{3.1}$$

Or simply

$$J_k = \int_\Gamma \left\{ W_s dy - t \frac{\partial u}{\partial x} \right\} d\Gamma \tag{3.2}$$

$$J_k = \int_\Gamma \left\{ W_s dy - t \frac{\partial u}{\partial x} \right\} d\Gamma \tag{3.3}$$

$$J_k = \int_\Gamma \left\{ W_s dx - t \frac{\partial u}{\partial y} \right\} d\Gamma \tag{3.4}$$

3.2 FIELD EQAUTION FOR SIFs

The displacement field equation in local coordinate system at crack tip written as [57]

$$u_i = \frac{1}{4\mu_1 \cosh(\pi\varepsilon)} \sqrt{\frac{r}{2\pi}} f_i(r, \theta, \varepsilon) \tag{3.5}$$

For K_I, f_1 and f_2 be defined as [57]

$$f_1 = D + 2\delta \sin\theta \sin\varphi \tag{3.6}$$

$$f_2 = -C - 2\delta \sin\theta \cos\varphi \tag{3.7}$$

For K_{II}, f_1 and f_2 be defined as

$$f_1 = -C + 2\delta \sin\theta \cos\varphi \tag{3.8}$$

$$f_2 = -D + 2\delta \sin\theta \sin\varphi \tag{3.9}$$

3.3 FINITE ELEMENT METHOD (FEM)

The FEM is basic to understand the further approach. To explain the basic of FEM. consider a 1-D body with domain Ω as shown in Figure 3.1 and discretize domain into sub-domains called elements $\{\Omega_1, \Omega_2, \Omega_3, \Omega_4\}$. Then at vertices of every element put nodes, having coordinates $x_i = \{x_1, x_2, x_3, x_4, x_5\}$ and associate the interpolation function ϕ_i to each nodes having support $w_i = \{w_1, w_2, w_3, w_4\}$ connected to every node.

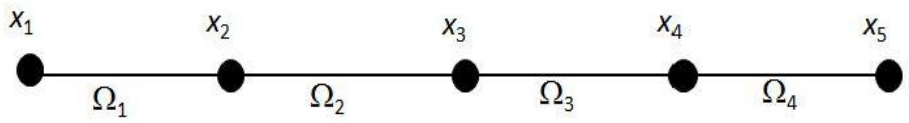

(a) Domain Ω discretization into sub domains

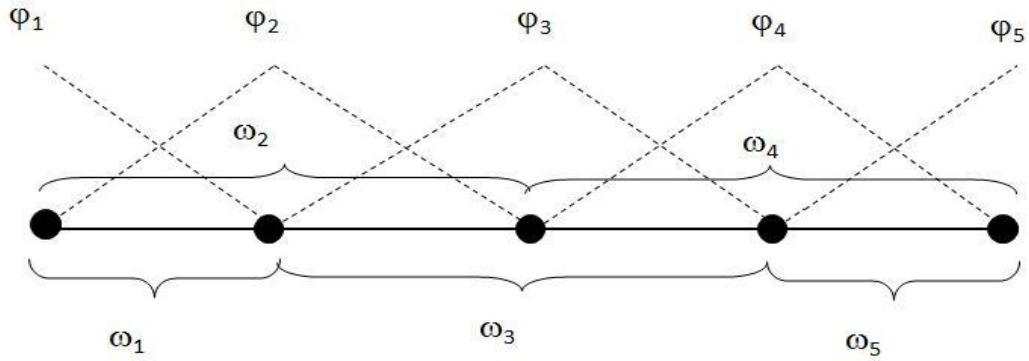

(b) Interpolation functions

Figure 3.1 FEM analysis [54]

The FEM approximation of local field is reads as [54]

$$u^h(X) = \sum_{i=1}^{i=4} \phi_i(X) u_i \tag{3.10}$$

To minimize the error $\left\| u - u^h \right\|_{w_i}$ select the interpolation function on support which satisfy the following condition $\sum_{i=1}^{i=n} \phi_i(X) = 1$

The characteristics of FEM approximation functions are

- When there is zero strain in element then displacement u_i at every node have constant value [54]

$$u^h(X)=\left(\sum_{i=1}^{i=n}\phi_i(X)\right)u_o=u_o \tag{3.11}$$

- The function interpolates in the value u_i, so the value at any point x_a

$$u^h(x_a)=\sum_{i=1}^{i=n}\phi_i(x_a)u_i=u_a \tag{3.12}$$

3.4 PUFEM

The basic thing in PU method is that the sum of shape function at each point is equal to unity in domain. Let us consider a body B in 1-D space having domain Ω as shown in Figure 3.2. By this method no meshing is required for approximation because nodes are placed arbitrarily in domain.

Let g_i be the local approximation of u in approximating $v_i(w_i)$ space defined on support w_i select g_i which can approximate the field u_i

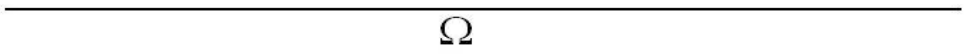

(a) Body with domain Ω

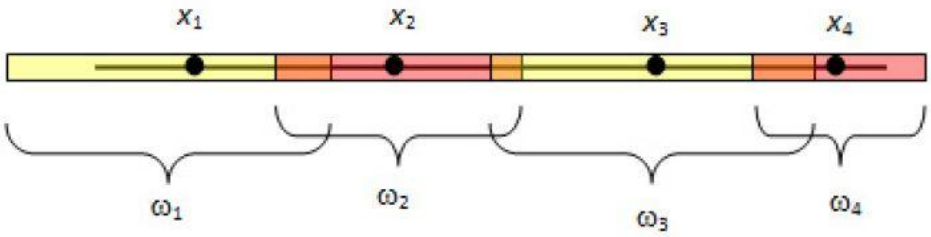

(b) Covering to the domain

Figure 3.2 Partition of unity method [54]

3.4.1 Methodology of partition of unity with in FEM

Implementations of both methods are same till discretization. To describe the difference consider the element Ω_3 with nodes x_3 and x_4 having shape function ϕ_3 and ϕ_4 which is union of $\{\Omega_2, \Omega_3\}$ and $\{\Omega_3, \Omega_4\}$ respectively as shown in Figure 3.3.

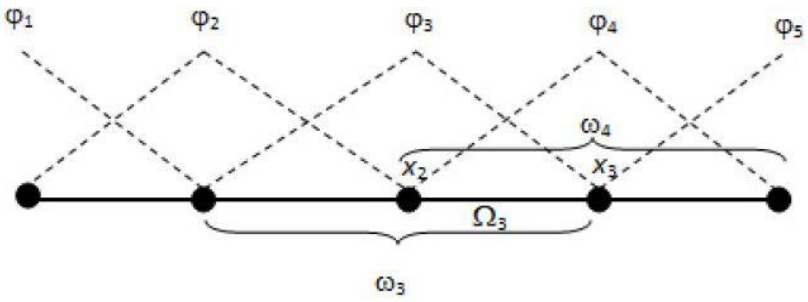

Figure 3.3 Interpolation functions on domain [54]

The basis function used to approximate the field U $\{\phi\} = \{\phi_3, \phi_4\} \times \{g_3, g_4\}$

3.5 XFEM

XFEM is classified from PUMs. As in partition of unity the domain is set of functions N_I satisfy the property as [55]

$$\sum_{I \in N^{fem}} N_I(x) = 1 \tag{3.13}$$

Where N^{fem} is the set of nodes as in FEM mesh. By using property the XFEM function modified by the product of PU function with So XFEM approximation is divided into standard and enriched part as [55]

$$\begin{aligned} u^h(x) &= u^h_{fem}(x) + u^h_{enr}(x) \\ u^h(x) &= \sum_{I \in N^{fem}} N_I(x) q_I + \sum_{J \in N^{ent}} N_J(x)[H(x) - H(x_J)]a_J \end{aligned} \tag{3.14}$$

Where $H(x_J)$ is the enrichment function at node *j*. This equation is used to get

$$\begin{bmatrix} K_{uu} & K_{ua} \\ K_{au} & K_{aa} \end{bmatrix} \begin{Bmatrix} q \\ a \end{Bmatrix} = \begin{Bmatrix} f_q \\ f_a \end{Bmatrix} \tag{3.15}$$

where K_{uu}, K_{ua} and K_{aa} are stiffness matrix of the standard FEM approximation, enriched approximation and for coupling respectively.

For the LEFM, functions used are and asymptotic functions for crack tip and jump function for displacement approximation through the crack face. The enriched approximation for LEFM as [55]

$$u^h(x) = \sum_{I \in N^{fem}} N_I(x) q_I + \sum_{J \in N^c} N_J(x) H(x) a_j + \sum_{K \in N^F} N_K(x) \sum_{\alpha=1}^{n} B_\alpha(r,\theta) b_K^\alpha \quad (3.16)$$

where N^c are the set of nodes cut by the crack interior and N^f are nodes cut by the crack tip field. H and B_α are the functions for crack surface and crack tip respectively, n is number of asymptotic function. a_J and b_K^α are the nodal degree of freedom corresponding to the basis function H and B_α, r and θ are the polar coordinates.

The equations for displacement field are global, but the enrichment functions are local because multiplied by nodal shape fucntions. There are four types of standard elements.

1. Split element are elements completely cut by the crack.
2. Tip elements have contain nodes of tip and within a fixed distance r_{enr}. Where r_{enr} is central crack tip radius. The nodes in this domain enriched by asymptotic functions.
3. Split-bending elements are neighbouring tip elements. These nodes are enriched by strongly and weakly functions.

The implementation of XFEM as below:

1. Representation of the interface: The discontinuity can be represented explicitly by lines or by using the LSM.

2. Selection of enriched nodes: For the case of local enrichment, only nodes closer to region of interest are taken in care of. The nodes for enrichment selected from the nodal values of level set function.

3. Choice of enrichment functions: There are different enrichment function can be used depending on the physics of the problem.

4. Integration: The standard gauss quadrature in elements enriched by discontinuous terms cannot be applied, because it implicitly assumes polynomial approximation.

3.6 NURBS USED FOR ANALYSIS

The framework of analysis based on NURBS consist followings features:

1. Product of knot vector is defined mesh for a NURBS patch is defined by.
2. The basis function supports consists small number of elements.
3. The control points with basis function defined geometry.
4. The coefficients of basis function are degree-of-freedom or control variable.

3.6.1 Derivative of NURBS basis function

For using NURBS basis function for analysis, derivative of basis function is must. For this derivative of equation (3.9) with respect of ξ is given below. [56]

$$\frac{d}{d\xi}R_i = w_i \frac{N_{i,p}(\xi)W(\xi)' - N_{i,p}(\xi)'W(\xi)}{(W(\xi))^2} \tag{3.17}$$

3.7 SPACE AND MAPPINGS

In conventional finite element method it has been work with different domains like physical mesh, physical element and parent domain. First and basic one is physical mesh which represents the actual geometry and represented with the help of nodes. The parent element is the space where we do integration by using Gaussian quadrature. To perform integration and get results from element first physical space mapped to same parent element and then reverse mapping to back after integration performed. The physical element is defined by using nodal coordinate and DOF are defined by the values of basis functions at nodes. These basis functions used to interpolate the nodes and also called as shape functions.

But other than classic finite element method, in IGA we are with different domains such as parameter space, Index space, physical mesh, control mesh, and the parent element.

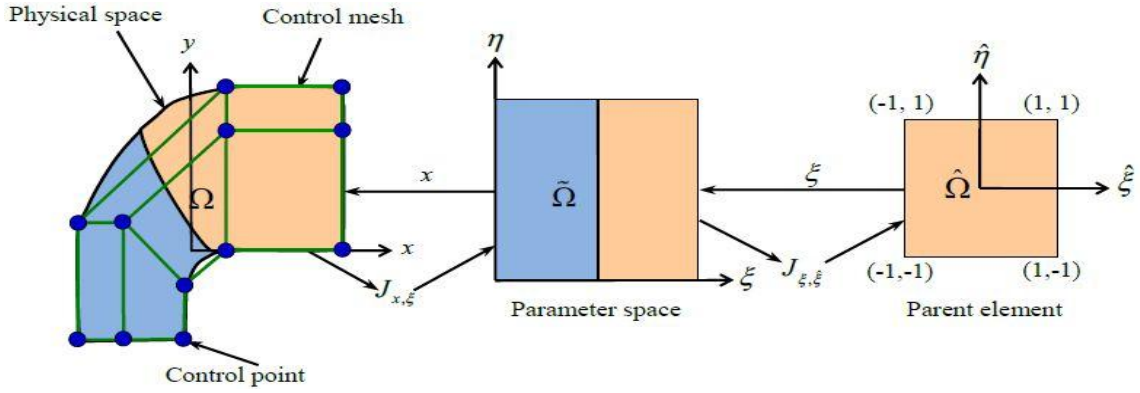

Figure 3.4 Mapping between spaces [31]

3.7.1 Physical space

The physical space as also described is where linear combination of basic functions represents the control points. These basis functions do not interpolate the control points. The physical is used to decompose the geometry and divided it into number of elements by the patches or knot spans.

A patch is a sub domain. Patches are curves in 1D, surfaces in 2D and volumes in 3D. Patches further divided into knot spans. Knot spans are bounded by knots. The basis functions are smooth inside the element and at the boundary of element having C^{p-m} continuity where m is multiplicity of knot and p is polynomial degree. Knot spans are smallest element.

3.7.2 Control mesh

The control mesh is defined by control points. Same as physical space it interpolates all the control points but do not equate to physical mesh. In 1D control mesh is straight line between points. In 2D it is quadrilaterals with four control points. In 3D element is tri linear hexahedral. The control mesh can be degenerated from quadrilateral to a triangle and may be arranged accordingly but physical mesh remains same.

3.7.3 Parameter space

The parameter space is the space where NURBS basis functions $R_{i,j}^{p,q}$ are defined for local elements are given by the knots. After defining basis functions in this space map the patch of elements into physical space. The elements of physical space are image as the same element in parametric space. The parametric space to the physical mapping is given by [56]

$$S(\xi,\eta)=\sum_{i=1}^{n}\sum_{j=1}^{m}R_{i,j}^{p,q}(\xi,\eta)B_{i,j} \tag{3.18}$$

3.7.4 Index space

Patching of each knot identified differently in index space. The space is under area [1,n+p+1] in the x direction and [1,m+q+1]in y direction thus the area is [1,n+p+1]×[1,m+q+1].

3.7.5 Parent element

The parent element has the constant area and that is the space in which we perform integration. We map $\hat{\xi}$ and $\hat{\eta}$ from ξ and η in the parent element for easily integrate the unknown using Gaussian quadrature. The parent to parameter space mapping is given by [56]

$$\xi(\bar{\xi}) = \frac{(\xi_{i+1} - \xi_i)\bar{\xi} + (\xi_{i+1} + \xi_i)}{2} \tag{3.19}$$

$$\eta(\bar{\eta}) = \frac{(\eta_{i+1} - \eta_i)\bar{\eta} + (\eta_{i+1} + \eta_i)}{2} \tag{3.20}$$

3.8 ISOGEOMETRIC FORMULATION FOR LINEAR PROBLEMS

3.8.1 Finite element discretization

We consider the boundary in physical space, the domains in parameter space and in parent element. The geometric mapping is the conversion of values of parameter domain to physical domain. We donate knot spans by $\Omega^{'e}$ in parametric space and Ω^e in physical space where *e* is taken from 1 to n_{el} (number of elements). There are knot spans which have zero value in it. So that takes the elements in the index space.

We consider number of basis functions represents as η_{np} which is same as the number of control points in space. R is the NURBS functions and $B^{cp} = [B_x^{cp} B_y^{cp}]$ the control points.

The mapping of x is given by [58]

$$x = \begin{bmatrix} x \\ \\ y \end{bmatrix} = \begin{bmatrix} \sum_{i=1}^{n_{np}} R_i(\xi,\eta) B_{x_i}^{cp} \\ \\ \sum_{i=1}^{n_{np}} R_i(\xi,\eta) B_{y_i}^{cp} \end{bmatrix} \tag{3.21}$$

In the weak form we calculate integration over the domain as sum of integrals at domain Ω_e

$$\sum_{e=1}^{n_{el}} \left\{ \int_{\Omega_e} (\nabla w^e)^T D^e \nabla u^e d\Omega - \int_{\Omega_e} w^{eT} b d\Omega \right\} = 0 \tag{3.22}$$

Let

$$\begin{aligned} u^e(x,y) &= R^e(\xi,\eta) d^e \\ w^e(x,y) &= R^e(\xi,\eta) w^e \\ b^e(x,y) &= R^e(\xi,\eta) b^e \end{aligned} \tag{3.23}$$

where

$$d^e = \left[u_{x1}^e u_{y1}^e u_{x2}^e u_{y2}^e ..... \right]^T \tag{3.24}$$

The notation $(*)^e_{x1}$ is represents the value at control point number 1. The element shape function is given for the element *e* in *x* direction. [55]

$$R_e = \begin{bmatrix} R_1^e & 0 & R_2^e & 0 & \dots \\ 0 & R_1^e & 0 & R_2^e & \dots \end{bmatrix} \tag{3.25}$$

The expression for strain as

$$\varepsilon^e = \begin{bmatrix} \varepsilon_{xx}^e \\ \varepsilon_{yy}^e \\ \gamma_x^e \end{bmatrix} = \nabla u^e = B^e d^e \tag{3.26}$$

Where B matrix

$$B^e = \nabla R^e = \begin{bmatrix} \frac{\partial R_1^e}{\partial x} & 0 & \frac{\partial R_2^e}{\partial x} & 0 \\ 0 & \frac{\partial R_1^e}{\partial y} & 0 & \frac{\partial R_2^e}{\partial y} \dots\dots \\ \frac{\partial R_1^e}{\partial y} & \frac{\partial R_1^e}{\partial x} & \frac{\partial R_2^e}{\partial y} & \frac{\partial R_2^e}{\partial x} \end{bmatrix} \tag{3.27}$$

Inserting the B matrix into equation (3.14) then we have [55]

$$\sum_{e=1}^{n_{el}} \left\{ \int_{\Omega_e} w^{eT} B^{eT} D^e B^e d^e d\Omega - \int_{\Omega^e} w^{eT} R^{eT} R^e b^e d\Omega \right\} = 0 \tag{3.28}$$

The element stiffness matrix as [55]

$$K^e = \int_{\Omega^e} B^{eT} D^e B^e d\Omega \tag{3.29}$$

3.9 SOLVING THE DISCRETE PROBLEM

For calculating the stiffness and force matrix first approximate the integral using Gaussian quadrature. To doing it first we have to map the parameter and physical space to parent element where we can perform integration. Let knot vectors $\Xi = \{\xi_1, \xi_2, \dots \xi_{n+p+1}\}$ and $\Gamma = \{\eta_1, \eta_2, \dots \eta_{m+q+1}\}$. From parent to parametric space the mapping is given by [55]

$$\xi = \begin{bmatrix} \xi(\hat{\xi}) \\ \eta(\hat{\eta}) \end{bmatrix} = \begin{bmatrix} \dfrac{(\xi_{i+1} - \xi_i)\hat{\xi} + (\xi_{i+1} + \xi_i)}{2} \\ \dfrac{(\eta_{i+1} - \eta_i)\hat{\eta} + (\eta_{i+1} + \eta_i)}{2} \end{bmatrix} \tag{3.30}$$

The Jacobian matrix is used to map parameter space to parent element is given by [55]

$$J(\hat{\xi}, \hat{\eta}) = \begin{bmatrix} \dfrac{\partial \xi}{\partial \hat{\xi}} & \dfrac{\partial \xi}{\partial \hat{\eta}} \\ \dfrac{\partial \eta}{\partial \hat{\xi}} & \dfrac{\partial \eta}{\partial \hat{\eta}} \end{bmatrix} = \begin{bmatrix} \dfrac{(\xi_{i+1} - \xi_i)\hat{\xi}}{2} & 0 \\ 0 & \dfrac{(\eta_{i+1} - \eta_i)\hat{\eta}}{2} \end{bmatrix} \tag{3.31}$$

To calculate the B matrix we have to know ∇R_i with respect to *x* and *y*. To find the expression for this we map the parameter space to physical space. The mapping *x* has the Jacobian matrix [55]

$$J_{x,\xi} = \begin{bmatrix} \dfrac{\partial x}{\partial \xi} & \dfrac{\partial x}{\partial \eta} \\ \dfrac{\partial y}{\partial \xi} & \dfrac{\partial y}{\partial \eta} \end{bmatrix} \tag{3.32}$$

With the inverse of matrix

$$\left(J_{x,\xi}\right)^{-1} = \begin{bmatrix} \dfrac{\partial \xi}{\partial x} & \dfrac{\partial \xi}{\partial y} \\ \dfrac{\partial \eta}{\partial x} & \dfrac{\partial \eta}{\partial y} \end{bmatrix} \tag{3.33}$$

We now let

$$\nabla = \begin{bmatrix} \dfrac{\partial}{\partial x} \\ \dfrac{\partial}{\partial y} \end{bmatrix} \text{ And } \hat{\nabla} = \begin{bmatrix} \dfrac{\partial}{\partial \xi} \\ \dfrac{\partial}{\partial \eta} \end{bmatrix} \tag{3.34}$$

Hence we have

$$\nabla = \left(J_{x,\xi}\right)^{-T} \hat{\nabla} \tag{3.35}$$

In above equation taking $G = \left(J_{x,\xi}\right)^{-T}$ get

$$\nabla R_i(x,y) = \begin{bmatrix} \frac{\partial R_i}{\partial x} \\ \frac{\partial R_i}{\partial y} \end{bmatrix} = \begin{bmatrix} \frac{\partial \xi}{\partial x} & \frac{\partial \eta}{\partial x} \\ \frac{\partial \xi}{\partial y} & \frac{\partial \eta}{\partial y} \end{bmatrix} \begin{bmatrix} \frac{\partial R_i(\xi,\eta)}{\partial \xi} \\ \frac{\partial R_i(\xi,\eta)}{\partial \eta} \end{bmatrix}$$
$$= \begin{bmatrix} \frac{\partial \xi}{\partial x} & \frac{\partial \eta}{\partial x} \\ \frac{\partial \xi}{\partial y} & \frac{\partial \eta}{\partial y} \end{bmatrix} \begin{bmatrix} \frac{\partial}{\partial \xi} \\ \frac{\partial}{\partial \eta} \end{bmatrix} R_i(\xi,\eta) = G\hat{\nabla} R_i(\xi,\eta) \tag{3.36}$$

For perform integration we have to know $J_{x,\xi}$ to map $\hat{\Omega}$ express as [55]

$$J_{x,\hat{\xi}} = \begin{bmatrix} \frac{\partial x}{\partial \bar{\xi}} & \frac{\partial x}{\partial \hat{\eta}} \\ \frac{\partial y}{\partial \bar{\xi}} & \frac{\partial y}{\partial \hat{\eta}} \end{bmatrix} = \begin{bmatrix} \frac{\partial x}{\partial \xi} & \frac{\partial x}{\partial \eta} \\ \frac{\partial y}{\partial \xi} & \frac{\partial y}{\partial \eta} \end{bmatrix} \begin{bmatrix} \frac{\partial \xi}{\partial \bar{\xi}} & \frac{\partial \xi}{\partial \hat{\eta}} \\ \frac{\partial \eta}{\partial \bar{\xi}} & \frac{\partial \eta}{\partial \hat{\eta}} \end{bmatrix} = J_{x,\xi} J_{\xi,\bar{\xi}} \tag{3.37}$$

We then express stiffness matrix as [55]

$$K^e = \int_{\Omega^e} B^{eT} D^e B^e d\Omega = \int_{-1}^{1}\int_{-1}^{1} B^{eT} D^e B^e \left| J_{x,\xi}{}^e \right| d\hat{\xi} d\hat{\eta} \tag{3.38}$$

$$K^e = \sum\sum B^{eT}\left(\xi\left(\hat{\xi}_i\right),\eta\left(\hat{\eta}_j\right)\right) D^e B^e\left(\xi\left(\hat{\xi}_i\right),\eta\left(\hat{\eta}_j\right)\right) \left| J_{x,\hat{\xi}}\left(\hat{\xi}_i,\hat{\eta}_j\right)\right| \rho_i \rho_j \tag{3.39}$$

3.10 ESSENTIAL BOUNDARY CONDITIONS

Due to Kronecker delta property then it's tough to apply boundary conditions. There are others method for boundary condition. Method of Lagrange multiplier adopted for imposition. It introduced new vector field λ^h

$$\lambda^h = \begin{Bmatrix} \lambda_u \\ \lambda_v \end{Bmatrix} = \begin{bmatrix} N_1 & 0 & \dots & N_{n\lambda} & 0 \\ 0 & N_1 & \dots & 0 & N_{n\lambda} \end{bmatrix} \begin{Bmatrix} \lambda_{u1} \\ \lambda_{v1} \\ . \\ \lambda_{un1} \\ \lambda_{vn1} \end{Bmatrix} = N(s)\lambda \tag{3.40}$$

where λ_i is Lagrange multiplier defined in a set of n_λ control point. Applying it to the weak equation

$$\int_{\Omega}(L\delta u)^{T}(DLu)d\Omega-\int_{\Omega}\delta u^{T}bd\Omega-\int_{\Gamma_t}\delta u^{T}td\Gamma=0 \tag{3.41}$$

The final equation is given as [56]

$$\begin{bmatrix} K & G \\ G^{T} & 0 \end{bmatrix}\begin{Bmatrix} u \\ \lambda \end{Bmatrix}=\begin{Bmatrix} f \\ q \end{Bmatrix} \tag{3.42}$$

3.11 SELECTION OF ENRICHED NODES

Interface represented by line segments, the following approaches has been used to select the nodes for enrichment when the crack surface has been represented by line segments

3.11.1 Strong or weak discontinuity

In order crack select displacement jump across represents the crack surface the nodes enrich with function H to or with function ψ to represent the weak discontinuity, an area criterion is used. Let the A1 and A2 are areas above and below the crack. A3 is the area of nodal support. If any of the ratio of A1/A3 or A2/A3, the node is removed from the set N^{c} is below a prescribed tolerance.

3.11.2 Crack tip enriched nodes

In the conventional XFEM, the support of enriched function as *h* goes to zero all the nodes of the enriched tip-elements with near-tip asymptotic fields.

3.11.3 Interface represented by level sets

When the crack surface is represented as a zero level set, the nodes for enrichment chose by determining the nodal.4 For bilinear quadrilateral element which is a two dimensional element with both global and local coordinates), if $\chi_{\min}\chi_{\max}\le 0$ and $\varphi_{\min}\varphi_{\max}\le 0$ then all nodes of enriched elements by tip asymptotic fields and tip lies within the element. If $\chi<0$ and $\varphi_{\min}\varphi_{\max}\le 0$, then nodes are enriched by Heaviside function and crack cuts through the element.

3.12 INTEGRATION

Partition of element into sub cells is one potential solution for numerical integration is. In these sub-cells the integrands are continuous and differentiable. Fig. shows sub-triangulation commonly used in XFEM which Sub-divided into triangles is used for integration. The approach has steps as follow

- Split the element into sub-cells aligned with discontinuity surface. The sub-cells are triangular usually
- Within the points of triangular quadrature integration is performed

Strong discontinuities and Singularity

Strong discontinuity: The enrichment function is chose to be Heaviside function H to model a strong discontinuity

$$H(x)=\begin{cases}+1 & x \;\; above \;\; the \;\; crack \;\; face \\ 0 & x \;\; below \;\; the \;\; crack \;\; face\end{cases} \tag{3.43}$$

The other choice of enrichment function is level set function

$$sign(\phi(x))=\begin{cases}+1 & x \;\; above \;\; the \;\; crack \;\; face \\ 0 & x \;\; below \;\; the \;\; crack \;\; face\end{cases} \tag{3.44}$$

There are modified Heaviside functions that eliminate sub-triangulation need for integration.

Singular fields: The near tip function is noted by $\{B_\alpha\}_{1\le\alpha\le4}$ and is given by

$$B_{1\le\alpha\le4}(r,\theta)=\sqrt{r}\left\{\sin\frac{\theta}{2},\cos\frac{\theta}{2},\sin\theta\sin\frac{\theta}{2},\sin\frac{\theta}{2}\cos\frac{\theta}{2}\right\} \tag{3.45}$$

Where (r,θ) are the crack tip polar coordinates which represents the near tip asymptotic fields. There are different formulations of tip function for different material.

3.13 Difficulties in the XFEM

As the method for incorporation in the FEM approximation basis permits arbitrary functions, the PU enrichment without changing the mesh have flexibility in modelling of boundary problems. The this method also have difficulties stated as below

- **Singular and discontinuous integrands** more care to integrate over enriched element is needed when approximation is discontinuous in element
- **The different partitions of unity blending** in conventional element the local enrichment is used leads to oscillation in the results for partially enriched elements.

- **Poor convergence rate** the convergence error of XFEM is remains in $\sqrt{h}$, where, h is element size.
- **SIF computation** XFEM requires post-processing for calculation of SIF value from computed displacement field.
- **Ill-conditioning** the additional DOF are introduced which further depend on enrichment functions. So requirement of more number of enrichment functions.

Numerical integration for enriched approximation: Generalized Gaussian quadrature

A quadrature in R^d is a formula of the form

$$\int_{\Omega} w(x) f(x) dx \approx \sum_{i=1}^{n} w_i f(x_i) \tag{3.46}$$

Where f is an integrand defined in this region, w is weight function. The points $x_i \in R^d$ are called quadrature weights and quadrature nodes. By using point-elimination scheme Newton's method, for triangular and square domains a new quadrature rule was proposed. This scheme also applied to the polygons and polyhedral called 'Generalized Gaussian quadrature'. The following steps to use this rule

- Find an initial quadrature for the integration region, appropriate weights and basis functions that satisfy equation
- Eliminate node with minimum significance
- Solve equation iteratively until convergence is attained. Until no nodes can be removed steps has been continued.

3.14 EXTENDED ISOGEOMETRIC ANALYSIS (XIGA)

The discretize form for the mechanical equation using in IGA can be written as [57]

$$Ku^h = F \tag{3.47}$$

where u^h displacement vector consists additional and standard DOF both [57]

$$u^h = \{u \quad a \quad b_1 \quad b_2\} \tag{3.48}$$

where additional degree of freedom is used to reproduce crack tip and faces fields, respectively. The mechanical force vector F and global stiffness matrix K is derived by assembly of their element [57].

$$K_{ij}^{ab} = \begin{bmatrix} K_{ij}^{ab} & K_{jj}^{ua} & K_{ij}^{ub} \\ K_{ij}^{au} & K_{ij}^{aa} & K_{ij}^{ab} \\ K_{ij}^{bu} & K_{ij}^{ba} & K_{ij}^{bb} \end{bmatrix} \tag{3.49}$$

$$f_i = \left\{ f_i^u \quad f_i^a \quad f_i^{b_1} \quad f_i^{b_2} \quad f_i^{b_3} \quad f_i^{b_3} \right\} \tag{3.50}$$

In mechanical loading the components of force vector and extended stiffness matrix are [57]

$$K^{rs} = \int_{\Omega^e} \left(B^r\right)^T D B^s d\Omega \tag{3.51}$$

$$f_i^u = \int_{\Gamma_t} N_i f^t d\Gamma + \int_{\Omega^e} N_i f^b d\Gamma \tag{3.52}$$

$$f_i^a = \int_{\Gamma_t} N_i H f^t d\Gamma + \int_{\Omega^e} N_i H f^b d\Gamma \tag{3.53}$$

$$f_i^{b_\alpha} = \int_{\Gamma_t} N_i F_\alpha f^t d\Gamma + \int_{\Omega^e} N_i F_\alpha f^b d\Gamma \tag{3.54}$$

where Γ =1,2,3 and 4 , f^b is the body force , D is the elasticity matrix, f^t is the external traction force, , N_i are NURBS basis functions and B^r are basis functions derivatives matrices and similarly the discretize for of thermal equation as [57]

$$QT^h + f^{th} = 0 \tag{3.55}$$

Where the $T^h = \{u \quad a \quad b_1\}$ and thermal stiffness matrix [57]

$$Q_{ij}^e = \begin{bmatrix} Q_{ij}^{ab} & Q_{ij}^{ua} & Q_{ij}^{ub} \\ Q_{ij}^{au} & Q_{ij}^{aa} & Q_{ij}^{ab} \\ Q_{ij}^{bu} & Q_{ij}^{ba} & Q_{ij}^{bb} \end{bmatrix} \tag{3.56}$$

$$f_i^{th-e} = \left\{ f_i^{th-u} \quad f_i^{th-a} \quad f_i^{th-b_1} \right\} \tag{3.57}$$

The components of force vector and thermal stiffness matrix defined as [57]

$$Q^{rs} = \int_{\Omega^e} \left(B^{th-r}\right)^T \kappa B^{th-s} d\Omega \tag{3.58}$$

$$f^{th-u} = \int_{\Gamma_q} N_i \bar{q} d\Gamma \tag{3.59}$$

$$f^{th-a} = \int_{\Gamma_q} N_i H \bar{q} d\Gamma \tag{3.60}$$

$$f^{th-b_1} = \int_{\Gamma_q} N_i F_\alpha \bar{q} d\Gamma \tag{3.61}$$

Where components of B matrix are as follow [57]

$$B_i^{th-u} = \begin{bmatrix} N_{i,x} \\ N_{i,y} \end{bmatrix} \tag{3.62}$$

$$B_i^{th-a} = \begin{bmatrix} (N_i H)_x \\ (N_i H)_y \end{bmatrix} \tag{3.63}$$

$$B_i^{th-b_1} = \begin{bmatrix} (N_i F_{th})_x \\ (N_i F_{th})_y \end{bmatrix} \tag{3.64}$$

$$\kappa = \begin{bmatrix} k_{11} & 0 \\ 0 & k_{22} \end{bmatrix} \tag{3.65}$$

After calculating thermal, the KU=f equation expressed force vector as [57]

$$f = f^{th-eq} + f^{mech.} = \int_{\Omega} B^T C \varepsilon^{th} d\Omega + f^{mech.} \tag{3.66}$$

Where B matrix is defined as follow [57]

$$B_i^u = \begin{bmatrix} N_{i,x} & 0 \\ 0 & N_{i,y} \\ N_{i,y} & N_{i,x} \end{bmatrix} \tag{3.67}$$

$$B_i^a = \begin{bmatrix} (N_i H)_x & 0 \\ 0 & (N_i H)_y \\ (N_i H)_y & (N_i H)_x \end{bmatrix} \tag{3.68}$$

$$B_i^b = \begin{bmatrix} B_i^{b_1} & B_i^{b_2} & B_i^{b_2} & B_i^{b_4} \end{bmatrix} \tag{3.69}$$

$$B_i^{b_\alpha} = \begin{bmatrix} (N_i F)_x & 0 \\ 0 & (N_i F)_y \\ (N_i F)_y & (N_i F)_x \end{bmatrix} \tag{3.70}$$

Where i=1, 2, 3 and 4

F and *H* are functions of tip and Heaviside respectively.

3.15 MODELING OF CRACKS IN XIGA

Basic concepts of XFEM are employed within the framework of IGA. In this approach the both fields for crack are added to standard approximation. [57]

$$u = u^{IGA} + u^{XIGA} = u^{IGA} + u^{tip} + u^{heaviside} \tag{3.71}$$

$$T = T^{IGA} + T^{XIGA} = T^{IGA} + T^{tip} + T^{heaviside} \tag{3.72}$$

For model discontinuity in both displacement and temperature fields the function is defined as

$$T^{heaviside} = \sum_{i \in n_s} N_i(x) H(x) \hat{a}_i \tag{3.73}$$

where n_s the set of Heaviside is enriched control points. This at point X is defined as [57]

$$H(X) = \begin{cases} +1 & if\ (X - X^l).e_n > 0 \\ -1 & otherwise \end{cases} \tag{3.74}$$

Where X^l is closest point of crack to the point X . Tip function part of enrichment reproduced the complex analytical crack tip field [57]

$$T^{tip} = \sum_{i \in T_p} N_i(x) \left(\sum_{k \in F} f_k(x) \hat{b}_{ik} \right) \tag{3.75}$$

Where T_p control is points set of crack tip functions f_k. These are initially derived from the asymptotic solution as defined earlier in equation (3.75).

3.16 INTERACTION INTEGRAL FOR MECHANICAL LOADING

The SIF (K_I and K_{II}) are defined in fracture mechanics part So taking those value which derived by using interaction energy integral approach to expressed the interaction integral in case of mechanical loading can be written as [57]

$$M^{(1,2)} = \int_A \left[\sigma_{ij}^1 \frac{\partial u_i^2}{\partial x_1} + \sigma_{ij}^2 \frac{\partial u_i^1}{\partial x_1} - W^{1,2}\delta_{ij} \right] \frac{\partial q}{\partial x_j} dA \tag{3.76}$$

$$W^{1,2} = \frac{1}{2}\left(\sigma_{ij}^1 \varepsilon_{ij}^2 + \sigma_{ij}^2 \varepsilon_{ij}^1\right) \tag{3.77}$$

where q is scalar weight function have value one at crack tip and zero at contour. σ^1, σ^2 and $\varepsilon^1, \varepsilon^2$ are auxiliary and actual Cauchy strain tensor and stress tensor respectively. $W^{1,2}$ Represent the strain energy density for actual and states.

Similarly, interaction integral for thermal loading can be defined as [57]

$$M^{(1,2)} = \int_A \left[\sigma_{ij}^1 \frac{\partial u_i^2}{\partial x_1} + \sigma_{ij}^2 \frac{\partial u_i^1}{\partial x_1} - W^{1,2}\delta_{ij} \right] \frac{\partial q}{\partial x_j} dA + \alpha \int_A \frac{\partial T}{\partial x_1} \sigma_{kk}^2 dA \tag{3.78}$$

Interaction integral under mixed mode for linear elastic problems loading is given by

$$M^{1,2} = \frac{2}{H}\left(K_I^1 K_I^2 + K_{II}^1 K_{II}^2\right) \tag{3.79}$$

Where, H=E (young's modulus)

3.17 Crack propagation rate

This rate is depends on ΔK and stress ratio R as [59]

$$\frac{da}{dN} = f\left(\Delta K, R\right) \tag{3.80}$$

The dependency on R is less as comparatively so

$$\frac{da}{dN} = f(\Delta K) \tag{3.81}$$

The Paris law is use to evaluate the rate

$$\frac{da}{dN} = Cf(\Delta K) \tag{3.82}$$

As we take the homogenous material aluminium the value of C is taken as

$$\frac{da}{dN} = 1.1\times10^{-11}(\Delta K)^{3.89} \tag{3.83}$$

CHAPTER 4

NUMERICAL RESULTS AND DISCUSSION

Every mechanical engineering component is subject to some motion or load which cause stresses in it as example turbine blades, engine parts etc. The generation of stresses is reason of fatigue failure and failure cause casualties. Thus, it's essential to do analysis of components to predict fatigue failure life. In this section, I will present analysis results of side edge and center crack in homogenous material using XIGA approach by taking mode-I loading. The modeling of crack is done by the PU enrichment under XIGA. The Heaviside enrichment function is used for model crack length and signed distance for interference. For integration used Gauss integration for basic and enriched nodes as explained in 3.12.1 in chapter 3. As explained in IGA method the NURBS basis function are used as same Lagrangian function in XFEM. The NURBS basis function is making effects on four control points in every direction.

4.1 CRACK GROWTH IN HOMOGENEOUS MATERIAL

In this section the fatigue growth in homogenous material is analyzed using both XFEM and XIGA. The edge crack within domain is subjected to a tensile load varying from $\sigma_{\min} = 0$ MPa to $\sigma_{\max} = 70$ MPa along a direction perpendicular to the crack. By using interaction integral method the value of SIF is calculated for crack and the procedure for calculation of fatigue life is explained in chapter 3

4.1.1 Edge crack growth

In a homogenous material plate in which fatigue growth analysis of crack with dimensions 50×50 having an edge crack. The crack of length a=10 is taken for convergence. The values of SIFs under mode-I loading using XIGA (for control net) and XFEM (for control mesh) are calculated as shown in Figure 4.2(a) and Figure 4.2(b). As shown in these plot the convergence of SIFs values in XIGA case is at control net 30 × 60 (1800 control points) and in case of XFEM for mesh size of 50 × 100 (5000 control points). The analytical value of SIF is calculated as [57]

$$K_{analytical} = f\sigma\sqrt{\pi a} \tag{4.1}$$

where, $f = 1.12 - 0.23(a/L) + 10.55(a/L)^2 - 21.72(a/L)^3 + 30.39(a/L)^4$

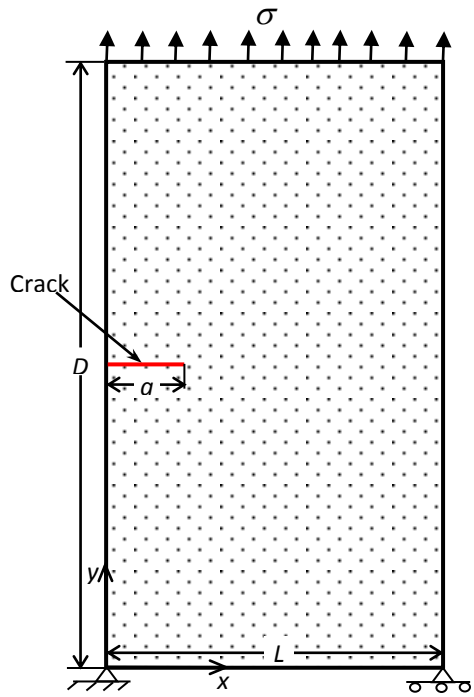

Figure 4.1 Edge cracked homogenous body with loading and boundary conditions

The value of SIF for XFEM having mesh size 50 × 100, XIGA having control net 30 × 60 and by analytical method given by Gdoduos in 2005 is shown in Figure 4.3. These results shows the values obtained by XFEM and XIGA are closed as by analytical method. The value of SIF is increased as respect to length of crack. The crack is start with the value of 5 mm and extended 2 mm in prediction direction. The value of SIF is calculated for new crack length until the final failure i.e. $K_{\text{Ieq}} \geq (K_{\text{IC}})_{m1}$ then simulation stop.

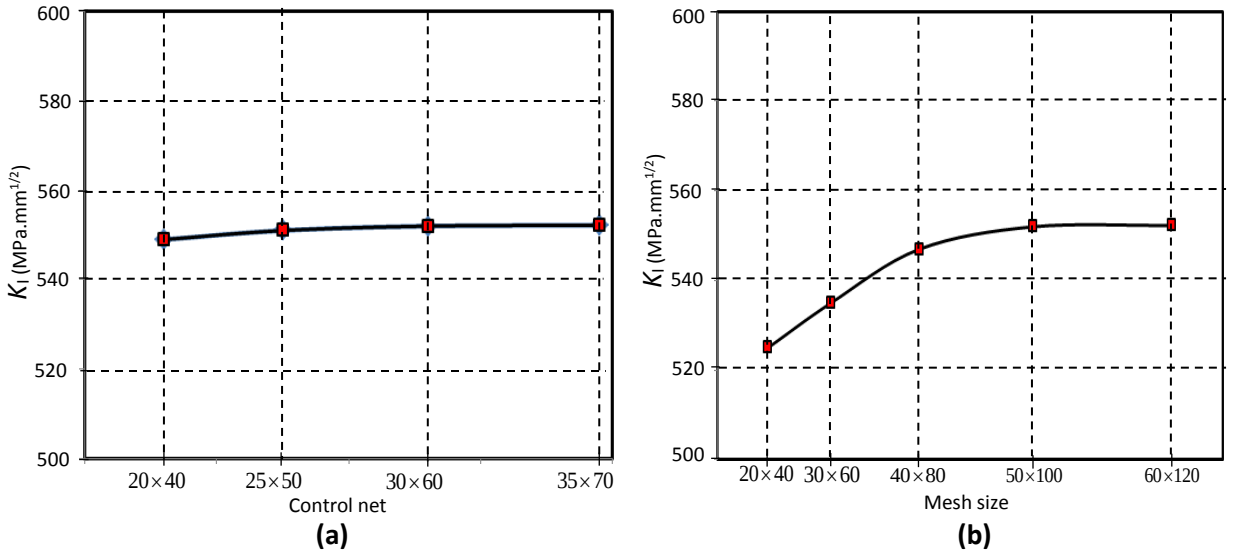

Figure 4.2 Convergence of (a) XIGA and (b) XFEM for in homogenous material having an edge crack

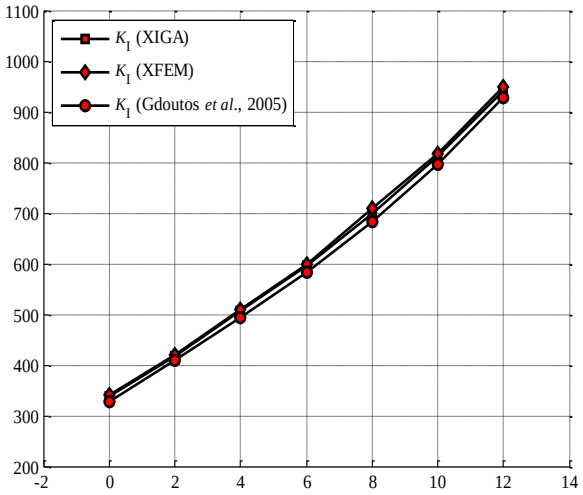

Figure 4.3 Variation of K_I value with crack extension for in homogenous material having an edge crack

Figure 4.4 shows that crack follows similar path. The contour plots of normal stress, σ_{yy} and strain, ε_{yy} obtained by XIGA for crack length of 5 initially mm is shown in Figure 4.5.

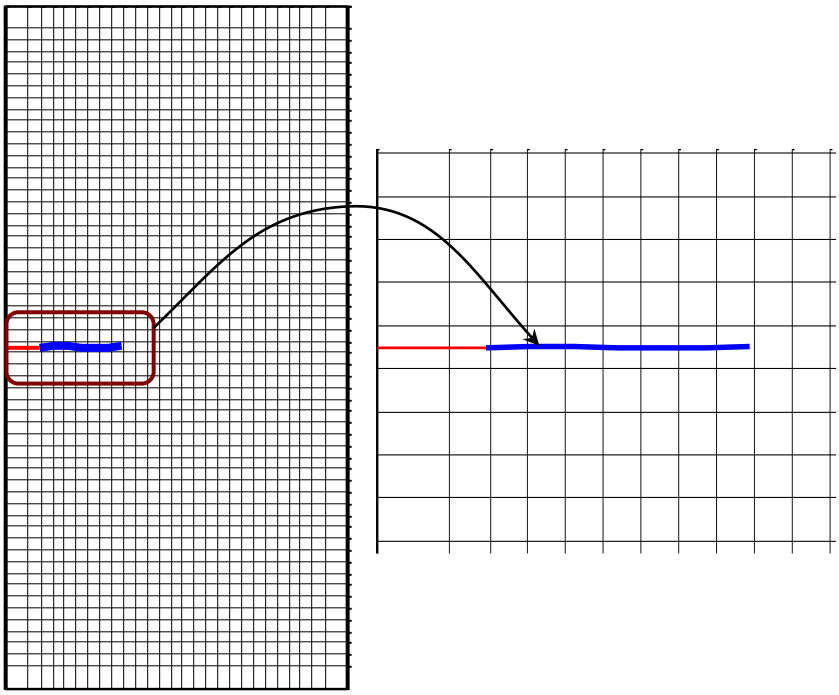

Figure 4.4 Crack growth path for an edge crack in homogenous material

4.1.2 Center crack growth

The center crack having crack length 2a is shown in the homogenous domain of 50 × 100. For taking crack length 20 mm the convergence is obtained by control net in case of XIGA and with

meshing in XFEM is shown in Figure 4.7. The convergence for the value of SIFs in these plots is obtained in XIGA case having control net of 30 × 60 (1800 control points) and in XFEM with mesh size 50 × 100 (5000 control points). The analytical formula for SIF for central crack is [57]

$$K_{analytical} = f\sigma\sqrt{\pi a} \tag{4.2}$$

where, $f = 1 + 0.128(a/L) - 0.288(a/L)^2 + 1.523(a/L)^3$

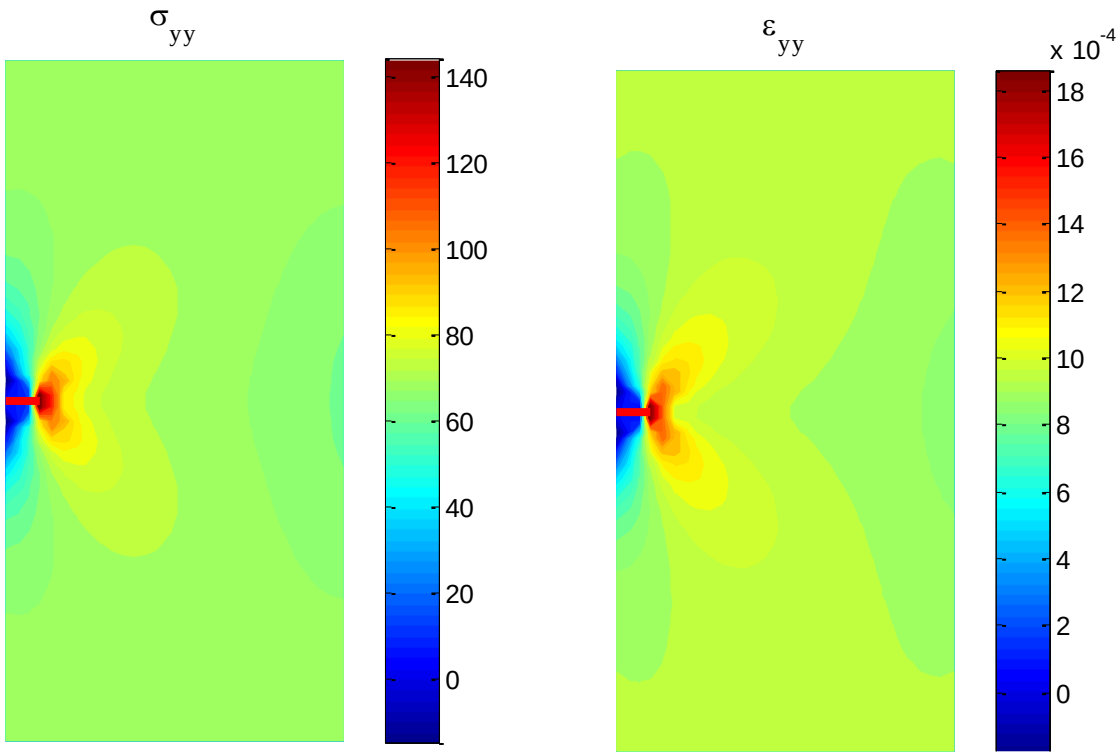

Figure 4.5 (a) Plot of σ_{yy} (MPa) for homogenous material having an edge crack, (b) Plot of ε_{xy} for homogeneous material having an edge crack

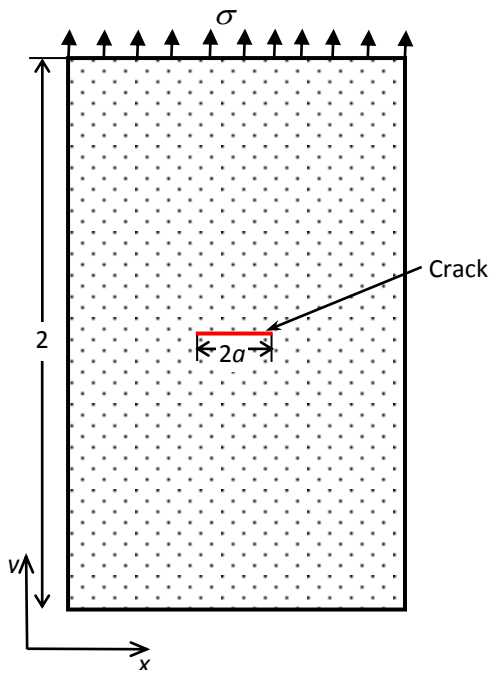

Figure 4.6 Center cracked homogenous body with boundary and loading conditions

The comparison of value of SIF calculated using XIGA (having control net 30 × 60), with XFEM (50 × 100 mesh size) and by analytical formula as respect to crack extension is shown in Figure 4.8. The results have good agreement by both XIGA and XFEM with analytical method. The SIF value is increased with the crack extension taken the crack length 2a=10mm. The extension of crack is increasing from 2mm to final failure point where simulation stops when $K_{\text{Ieq}} \geq (K_{\text{IC}})_{m1}$. The contour plots of normal stress, σ_{yy} and strain, ε_{yy} for crack length of 5 mm initially obtained by XIGA is shown in Figure 4.10.

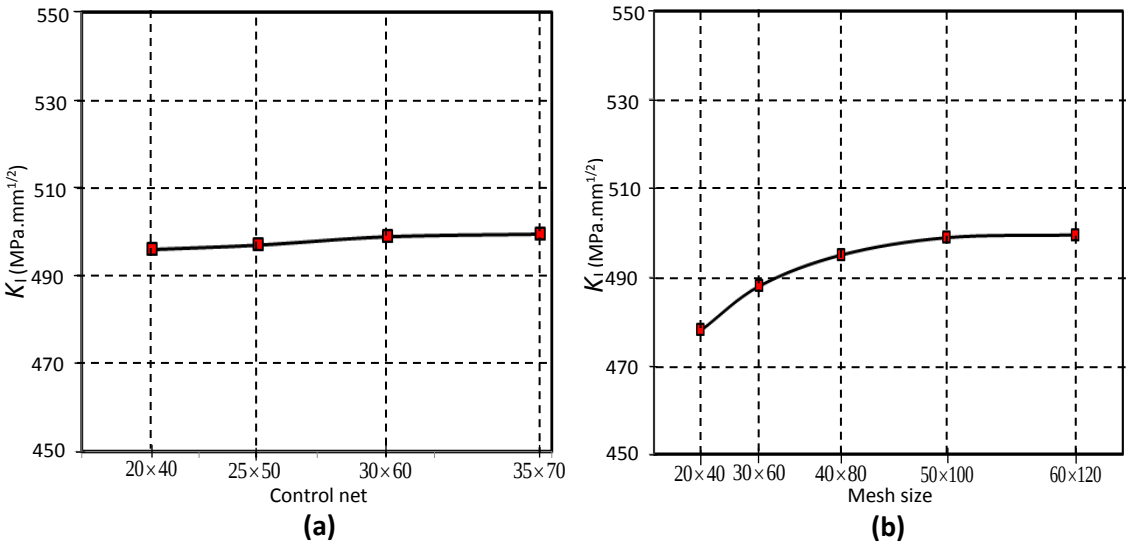

Figure 4. 7 Convergence of (a) XIGA and (b) XFEM for homogenous material having center crack

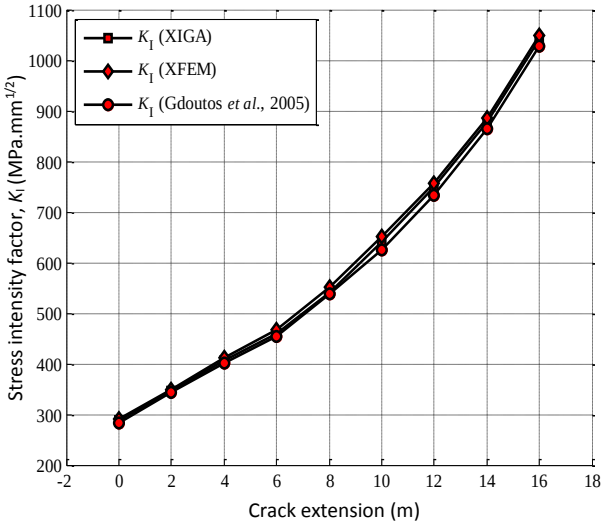

Figure 4.8 variation of K_I with crack extension for homogenous material having Centre crack

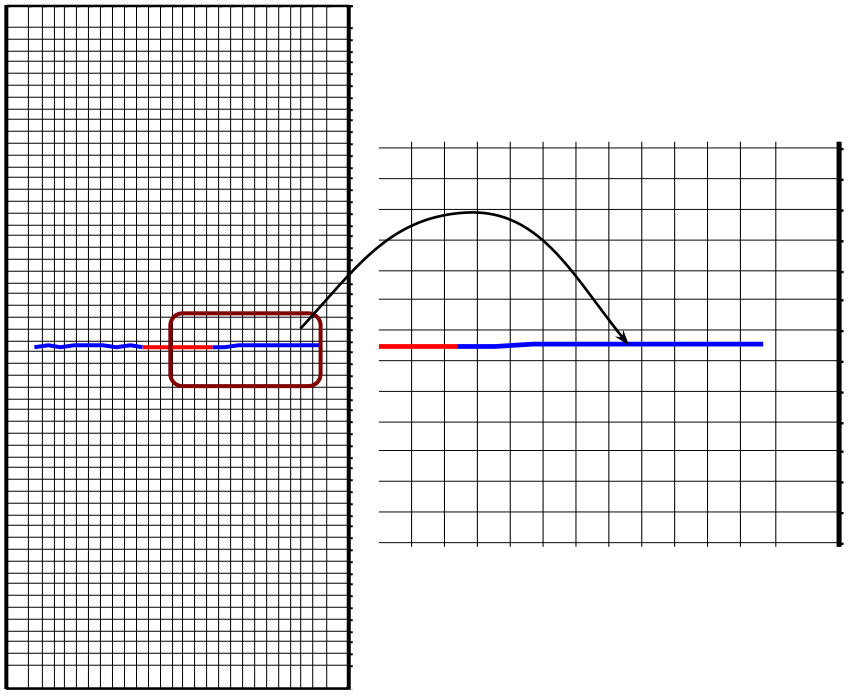

Figure 4.9 Crack growth path for a center crack in homogenous material

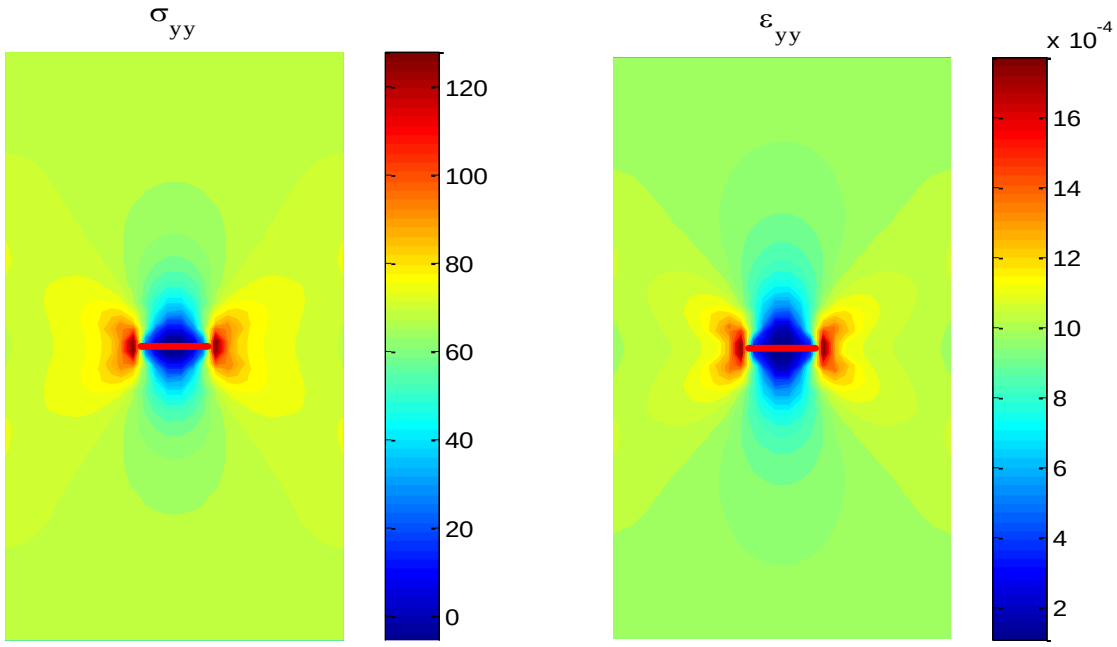

Figure 4.10 (a) Plot of σ_{yy} (MPa) for homogenous material having center crack, (b) Plot of ε_{yy} for homogenous material having center crack.

CHAPTER 5

5.1 CONCLUSION

In this thesis work, extrinsic partition of unity enriched XIGA and XFEM have been successfully used to perform analysis of crack growth for center crack or an edge crack in homogenous material under mode-I loading. In IGA, NURBS basis functions are used for the solution and for defining the geometry. The NURBS as basis functions with higher order continuity provides smooth solution.

- Both XIGA and XFEM have been successfully used for the modeling of crack growth problems in homogenous material, bi-material, FGM and bi-layered FGM. The results come by XIGA by using coarse control net of 30×60 are found in well accord with results generated by a fine mesh size of 50×100 using XFEM. Moreover, the outcomes generated by XIGA and XFEM are found in good accord with the analytical solutions.
- The effect of edge crack is more dominant than center crack under mechanical loading

5.2FUTURE SCOPE

The present work deals with crack growth analysis in homogenous under plane stress condition. This work can be extended further for the following cases,

- Crack growth analysis in bi-materials, FGMs and bi-layered FGMs.
- Analysis of crack growth in the presence of defects like holes and inclusions in bi-materials, FGMs and bi-layered FGMs.
- Fatigue crack growth study in 3-D fracture problems can be performed.
- Crack branching and crack interaction phenomena can be investigated.
- Multi-scale approach of crack growth for the simulation can be developed in homogenous, bi-material, FGM and bi-layered FGM.
- Crack growth study in power plant components can be performed under thermo-mechanical loading.
- Analysis of composites and smart materials can be performed for the understanding of their fracture and failure mechanism.
- Effect of defects of composites and smart materials on the fatigue life can be analyzed.

- Nonlinear analysis of fatigue crack growth can be performed in homogenous, bi-material, FGM and bi-layered FGM.
- Nonlinear analysis of fatigue crack growth can be performed in homogenous, bi-material, FGM and bi-layered FGM in presence of defects.
- Vibration analysis of cracked homogenous, FGM, laminated composite, sandwich and piezoelectric plates can be performed.
- Buckling analysis of cracked homogeneous, FGM, laminated composite, sandwich and piezoelectric plates can be performed.
- Parallel algorithms can be developed to reduce the overall computational

REFERENCES

[1] Swenson, D. V., and Ingraffea, A. R. (1988). "Modeling mixed-mode dynamic crack propagation using finite elements: theory and applications" . *Computational Mechanics*, Vol.*3*(6), pp.381-397.

[2] Belytschko, T., Krongauz, Y., Organ, D., Fleming, M., and Krysl, P. (1996). "Meshless methods: an overview and recent developments", *Computer Methods in Applied Mechanics and Engineering*, Vol.*139*(1-4), pp.3-47.

[3] Hughes, T. J., Cottrell, J. A., and Bazilevs, Y. (2005). "Isogeometric analysis: CAD, finite elements, NURBS, exact geometry and mesh refinement". *Computer Methods in Applied Mechanics and Engineering*, Vol.*194*(39-41), pp.4135-4195.

[4] Bazant, Z. P., and Planas, J. (1997). "*Fracture and Size Effect in concrete and other quasi brittle materials"* Vol.16. CRC press.

[5] Griffith, A.A. (1924),"The theory of rupture"*, First International Congress of Applied Mechanics,* Delft, Vol.19, pp.55-63;

[6] Griffith, A.A.(1921) "The phenomena of rupture and flow in solids*, Philosofical Transactions"*, *Series A*, Vol.221. pp.163-198;

[7] Westergaard, H. M. (1939). "Bearing pressures and cracks". *Journal of Applied Mechanics*, Vol.*6*(2), pp.A49-A53.

[8] Irwin, L.H, Ingraffea, A. R., and Castel M.L. (2000). "Fatigue crack growth in pavements". *Journal of Transportation Engineering*, Vol.*126*(4), pp.283-290.

[9] Wells, G. N., Alfaiate, J., and Sluys, L. J. (2002). "On the use of embedded discontinuity elements with crack path continuity for mode-I and mixed-mode fracture". *Engineering Fracture Mechanics*, Vol.*69*(6), pp.661-686.

[10] Rice, J. (1988). "Elastic fracture mechanics concepts for interfacial cracks." *Journal of Applied Mechanics*, Vol.*55*(1), pp.98-103.

[11] Barsoum, R. S. (1976). "On the use of isoparametric finite elements in linear fracture mechanics". *International Journal for Numerical Methods in Engineering*, *10*(1), 25-37.

[12] Fawkes, A. J., Owen, D. R. J., and Luxmoore, A. R. (1979). "An assessment of crack tip singularity models for use with isoparametric elements". *Engineering Fracture Mechanics*, *11*(1), 143-159.

[13] Beissel, S., and Belytschko, T. (1996). "Nodal integration of the element-free Galerkin method". *Computer Methods in Applied Mechanics and Engineering*, *139*(1-4), 49-74.

[14] Koh, H. M., Lee, H. S., and Haber, R. B. (1988). "Dynamic crack propagation analysis using Eulerian-Lagrangian kinematic descriptions". *Computational Mechanics*, Vol.*3*(3), pp.141-155.

[15] Kanninen, M. F. (1974). "A dynamic analysis of unstable crack propagation and arrest in the DCB test specimen". *International Journal of Fracture*, Vol.*10*(3), pp.415-430.

[16] Swenson, D. V., and Ingraffea, A. R. (1988). "Modeling mixed-mode dynamic crack propagation using finite elements: theory and applications." *Computational Mechanics*, Vol.*3*(6), pp.381-397.

[17] Belytschko, T., Lu, Y. Y., and Gu, L. (1994). "Element-free Galerkin methods." *International Journal for Numerical Methods in Engineering*, Vol.*37*(2), pp.229-256.

[18] Gifford Jr, L. N., and Hilton, P. D. (1978). "Stress intensity factors by enriched finite elements." *Engineering Fracture Mechanics*, Vol.*10*(3), pp.485-496.

[19] Belytschko, T .,Budyn, E., Zi, G., and Moes, N.. (2004). "A method for multiple crack growth in brittle materials without remeshing". *International Journal for Numerical Methods in Engineering*, *61*(10), 1741-1770.

[20]Belytschko, T., and Black, T. (1999). “Elastic crack growth in finite elements with minimal remeshing”. *International Journal for Numerical Methods in Engineering*, Vol.*45*(5), pp.601-620.

[21]Liu, H., Al-Mahaidi, R., and Zhao, X. L. (2009). “Experimental study of fatigue crack growth behaviour in adhesively reinforced steel structures”. *Composite Structures*, Vol.*90*(1), pp.12-20.

[22]Oden, J. T., and Duarte, C. A. (1997). “Clouds, cracks and FEM’s”. *Recent Developments in Computational and Applied Mechanics*, Vol.302-321.

[23]Strouboulis, T., Copps, K., and Babuska, I. (2000). “The generalized finite element method: an example of its implementation and illustration of its performance”. *International Journal for Numerical Methods in Engineering*, Vol.*47*(8), pp.1401-1417.

[24]Fleming, M., Chu, Y. A., Moran, B., and Belytschko, T. (1997). “Enriched element-free Galerkin methods for crack tip fields”. *International Journal for Numerical Methods in Engineering*, Vol.*40*(8), pp.1483-1504.

[25]Strouboulis, T., Copps, K., and Babuska, I. (2001). “The generalized finite element method”. *Computer Methods in Applied Mechanics and Engineering*, Vol.*190*(32-33), pp.4081-4193.

[26]Belytschko, T., and Black, T. (1999). “Elastic crack growth in finite elements with minimal remeshing”. *International Journal for Numerical Methods in Engineering*, Vol.*45*(5), pp.601-620.

[27]Moes, N., Dolbow, J., and Belytschko, T. (1999). “A finite element method for crack growth without remeshing”. *International Journal for Numerical Methods in Engineering*, Vol.*46*(1), pp.131-150.

[28]Sukumar, N., Moes, N., Moran, B., and Belytschko, T. (2000). “Extended finite element method for three-dimensional crack modeling”. *International Journal for Numerical Methods in Engineering*, Vol.*48*(11), pp.1549-1570.

[29]Stolarska, M., Chopp, D. L., Moes, N., and Belytschko, T. (2001). “Modelling crack growth by level sets in the extended finite element method”. *International Journal for Numerical Methods in Engineering*, Vol.*51*(8), pp.943-960.

[30]Osher, S., and Fedkiw, R. (2003). “Implicit Functions”. In *Level Set Methods and Dynamic Implicit Surfaces* pp. 3-16

[31]Sukumar, N., Chopp, D. L., and Moran, B. (2003). “Extended finite element method and fast marching method for three-dimensional fatigue crack propagation”. *Engineering Fracture Mechanics*, Vol.*70*(1), pp.29-48.

[32]Moes, N., and Belytschko, T. (2002). “Extended finite element method for cohesive crack growth”. *Engineering Fracture Mechanics*, Vol.*69*(7), pp.813-833.

[33]Zi, G., and Belytschko, T. (2003). “New crack-tip elements for XFEM and applications to cohesive cracks”. *International Journal for Numerical Methods in Engineering*, Vol.*57*(15), pp.2221-2240.

[34]Meschke, G., and Dumstorff, P. (2007). “Energy-based modeling of cohesive and cohesionless cracks via X-FEM”. *Computer Methods in Applied Mechanics and Engineering*, Vol.*196*(21-24), pp.2338-2357.

[35]Schramm, U., and Pilkey, W. D. (1993). “The coupling of geometric descriptions and finite elements using NURBs, A study in shape optimization”. *Finite Elements in Analysis and Design*, Vol.*15*(1), pp.11-34.

[36]Hughes, T. J., Cottrell, J. A., and Bazilevs, Y. (2005). “Isogeometric analysis: CAD, finite elements, NURBS, exact geometry and mesh refinement”. *Computer Methods in Applied Mechanics and Engineering*, Vol.*194*(39-41), pp.4135-4195.

[37]Wall, W. A., Frenzel, M. A., and Cyron, C. (2008). “Isogeometric structural shape optimization”. *Computer Methods in Applied Mechanics and Engineering*, Vol.*197*(33-40), pp.2976-2988.

[38]Manh, T., and Lee, J. (2014). “Stacking sequence optimization for maximum strengths of laminated composite plates using genetic algorithm and isogeometric analysis”. *Composite Structures*, Vol.*116*, pp.357-363.

[39]Uhm, T. K., and Youn, S. K. (2009). “T-spline finite element method for the analysis of shell structures”. *International Journal for Numerical Methods in Engineering*,Vol.*80*(4), pp.507-536.

[40]Ghorashi, S. S., Valizadeh, N., Mohammadi, S., and Rabczuk, T. (2012). “Extended isogeometric analysis of plates with curved cracks”. In *Proceedings of the Eighth International Conference on Engineering Computational Technology, Civil-Comp Press, Stirlingshire, UK*.

[41]Luycker De , Benson, D. J., Bazilevs, Y., , E., Hsu, M. C., Scott, M., Hughes, T. J. R., and Belytschko, T. (2010). “A generalized finite element formulation for arbitrary basis functions: from isogeometric analysis to XFEM”. *International Journal for Numerical Methods in Engineering*, Vol.*83*(6), pp.765-785.

[42]Wilson, W. K., and Yu, I. W. (1979). “The use of the J-integral in thermal stress crack problems”. *International Journal of Fracture*, Vol.*15*(4), pp.377-387.

[43]Prasad, N. N. V., Aliabadi, M. H., and Rooke, D. P. (1994). “The dual boundary element method for thermoelastic crack problems”. *International Journal of Fracture*, Vol.*66*(3), pp.255-272.

[44]Hosseini, S. S., Bayesteh, H., and Mohammadi, S. (2013). “Thermo-mechanical XFEM crack propagation analysis of functionally graded materials”. *Materials Science and Engineering: A*, Vol.*561*, pp.285-302.

[45]Mohammadi, S. (2012). *“XFEM fracture analysis of composites”*. John Wiley and Sons Incorporated.

[46]Cottrell, J. A., Reali, A., Bazilevs, Y., and Hughes, T. J. (2006). “Isogeometric analysis of structural vibrations”. *Computer Methods in Applied Mechanics and Engineering*, Vol.*195*(41-43), pp.5257-5296.

[47]Wall, W. A., Frenzel, M. A., and Cyron, C. (2008). “Isogeometric structural shape optimization”. *Computer Methods in Applied Mechanics and Engineering*, *197*(33-40), 2976-2988.

[48]Borden J.A., Schillinger, D., Dede, L., Scott, M. A., Evans, M. J., Rank, E., and Hughes, T. J. (2012). “An isogeometric design-through-analysis methodology based on adaptive hierarchical refinement of NURBS, immersed boundary methods, and T-spline CAD surfaces”. *Computer Methods in Applied Mechanics and Engineering*, Vol.*249*, pp.116-150.

[49]Ghorashi, S. S., Valizadeh, N., Mohammadi, S., and Rabczuk, T. (2012). “Extended isogeometric analysis of plates with curved cracks”. In *Proceedings of the Eighth International Conference on Engineering Computational Technology, Civil-Comp Press, Stirlingshire, UK*.

[50]Singh, I. V., Bhardwaj, G., and Mishra, B. K. (2015). “A new criterion for modeling multiple discontinuities passing through an element using XIGA”. *Journal of Mechanical Science and Technology*, Vol.*29*(3), pp.1131-1143.

[51]Gracie, R., Belytschko, T., and Ventura, G. (2009). “A review of extended/generalized finite element methods for material modeling”. *Modeling and Simulation in Materials Science and Engineering*, Vol.*17*(4), pp.043001.

[52]Borden, M. J., Verhoosel, C. V., Scott, M. A., Hughes, T. J., and Landis, C. M. (2012). “A phase-field description of dynamic brittle fracture”. *Computer Methods in Applied Mechanics and Engineering*, Vol.*217*, pp.77-95.

[53]Morganti, S., Auricchio, F., Benson, D. J., Gambarin, F. I., Hartmann, S., Hughes, T. J. R., and Reali, A. (2015). “Patient-specific isogeometric structural analysis of aortic valve closure”. *Computer Methods in Applied Mechanics and Engineering*, Vol.*284*, pp.508-520.

[54]Ahmed, A. (2009). “Extended finite element method (XFEM)-modeling arbitrary discontinuities and failure analysis”. *Istituto Universitario Di Studi Superiori Di Pavia*.

[55]McNary, M. (2009). “*Implementation of the extended finite element method (XFEM) in the abaqus software package”.* (Doctoral dissertation, Georgia Institute of Technology).

[56]Cottrell, J. A., Hughes, T. J., and Bazilevs, Y. (2009). *Isogeometric Analysis: Toward Integration of CAD and FEA*. John Wiley and Sons.

[57]Bayesteh, H., Afshar, A., and Mohammdi, S. (2015). “Thermo-mechanical fracture study of inhomogeneous cracked solids by the extended isogeometric analysis method”. *European Journal of Mechanics-A/Solids*, Vol.*51*, pp.123-139.

[58]Raknes, S. B. (2011). “Isogeometric Analysis and Degenerated Mappings” (Master's thesis, Institutt for matematiske fag).

[59]Kumar, P., & Prashant, K. (2009). *Elements of fracture mechanics*. Tata McGraw-Hill Education.